

Masterarbeit

zur Erlangung des akademischen Grades Diplom-Ingenieur (Dipl.-Ing./DI) im Studiengang „Industrieller Umweltschutz, Entsorgungstechnik und Recycling“ an der Montanuniversität Leoben

Schwermetallmobilisierung aus der Uranlagerstätte Bessines-sur-Gartempe

erstellt in Kooperation mit der

**Mines ParisTech, Centre de Géoscience/Hydrodynamique et
Réactions**

Vorgelegt von:

Anna-Katharina Erlacher BSc

0535268

Betreuer:

em.O.Univ.-Prof. DI. Dr.techn. K. Lorber

Dr. V. Lagneau

Dr.rer.nat. Dipl.-Min. D. Höllen

Leoben, 12.11.2013

EIDESSTATTLICHE ERKLÄRUNG

Ich erkläre an Eides statt, dass ich diese Arbeit selbständig verfasst, andere als die angegebenen Quellen und Hilfsmittel nicht benutzt und mich auch sonst keiner unerlaubten Hilfsmittel bedient habe.

Datum

Anna-Katharina Erlacher

AFFIDAVIT

I declare in lieu of oath, that I wrote this thesis and performed the associated research myself, using only literature cited in this volume.

Acknowledgment

I acknowledge, with gratitude, my debt of thanks to Dr. Vincent Lagneau for his advice, encouragement and patience. I owe sincere and earnest thankfulness to em. O.Univ.-Prof. Dipl.-Ing. Dr.techn. Karl Lorber and Dr. Emmanuel Ledoux. This master thesis would not have been possible unless the help and endurance of my supervisor Dr.rer.nat. Dipl.-Min. Daniel Höllen.

I would like to thank Nelly Martineau for her service in the laboratory and her help in word and deeds afterwards.

Special thanks to Hannah Kunodi and Stephan Hufnagl for their proofreading of my work.

It gives me immense pleasure to thank my family who supported and motivated me wherever they could.

At last I would like to thank Alina Gucher being there for me and Bibiane Schmoczer and Mario Löffler for giving accommodation during the last steps for my master thesis while staying in Leoben.

Kurzfassung

Schwermetallmobilisierung aus der Uranlagerstätte

Bessines-sur-Gartempe

Frankreich hat in der zweiten Hälfte des zwanzigsten Jahrhunderts intensiv Bergbau betrieben. Zu Beginn des neuen Jahrtausends wurde die letzte Uranmine in Jouac geschlossen. Die Nachsorge der Uranminen in Frankreich wurde der Firma AREVA SA übertragen. Diese kümmert sich nicht nur um die Einhaltung der Grenzwerte sondern auch um die Vorsorge potentieller Umweltauswirkungen. Im Rahmen der Masterarbeit wurden Wasserproben einer stillgelegten Uranmine im Limousin (Bessines-sur-Gartempe) durch vorhandene Pegel aus dem Grundwasserkörper entnommen. Im Labor wurden diese Proben mittels AAS, Emanometrie, IC und ICP chemisch analysiert. Zusätzlich wurde eine Simulation mithilfe des hydrodynamischen Programms HYTEC entwickelt. Dieses Programm modelliert die Ausbreitung chemischer Elemente sowie Mineralien im Grundwasser. Die Ergebnisse zeigen erhöhte Sulfat und Schwermetallgehalte, wobei die Uran und Radiumgehalte teilweise über den Grenzwerten für die Direkteinleitung in den Vorfluter liegen. Die Simulation zeigt, dass es durch die Oxidation von Pyrit zu einem Absinken des pH Wertes kommt, was zu einer Freisetzung von Schwermetallen führt.

Abstract

Heavy Metal Mobilisation of the uranium deposit

Bessines-sur-Gartempe

France had a significant mining activity during the second half of the 20th century, until the closing of the last uranium mine Jouac in 2001. The aftercare of mines was entrusted to AREVA SA. It includes arrangements for limiting and controlling discharges and impacts from them. This master thesis focuses on the effluent of a former uranium deposit in Limousin (Bessines-sur-Gartempe). At a field campaign water samples were taken out of existing piezometers. These water samples were analyzed to obtain their chemical composition by AAS, Emanometry, IC and ICP. At last step a simulation with the hydrodynamic program HYTEC was done. With this model the spreading of chemical elements and minerals in the groundwater for further ten years is described. The results show elevated levels of sulfate and several heavy metals. Uranium and radium values are often above the limits for a direct discharge into the receiving watercourse. The simulation shows that oxidation of pyrite causes a decrease in pH which leads to a release of heavy metals.

Abrégé

La Mobilisation des Métaux Lourds du Gisement d'Uranium

Bessines-sur-Gartempe

La France a connu une activité d'exploitation minière importante au cours de la seconde moitié du XX^e siècle, jusqu'à la fermeture de la dernière mine d'uranium à Jouac en 2001. La gestion de l'après-mine de l'ensemble des exploitations a été confiée à AREVA SA. Elle comprend des mesures de limitation des rejets, ainsi qu'un contrôle des rejets et des impacts. Le projet de fin d'études se concentre sur l'étude des rejets d'une ancienne mine d'uranium du Limousin (Bessines-sur-Gartempe). Pendant une campagne de terrain des échantillons de l'eau étaient pris. L'analyse des échantillons doit permettre de caractériser leur composition chimique. L'analyse était faite avec les méthodes AAS, Emanométrie, IC et ICP. Afin de contribuer la répartition d'éléments chimique et des minéraux dix ans à l'avance, un modèle hydrodynamique a été conçu par le biais du programme de simulation HYTEC. Les résultats montrent les valeurs élevées de sulfate et plusieurs métaux lourds. Les valeurs d'uranium et de radium sont souvent au-delà de la limite pour un déversement direct des eaux dans l'exutoire. La simulation montre que l'oxydation de pyrite cause une diminution des valeurs pH. Il apparaît une mobilisation de métaux lourds.

Table of Contents

	Page
1. INTRODUCTION.....	3
1.1 The Elements Uranium and Radium	3
1.2 Classification of uranium deposits [6].....	4
1.3 Uranium Mining worldwide	5
1.4 Legal Framework [8]	6
1.5 Uranium Mining in France [9].....	9
1.6 Uranium Mining in Germany [11]	10
1.6.1 Uranium Mining in Schlema-Alberode [12].....	10
2. THE URANIUM DEPOSIT BESSINES-SUR-GARTEMPE	12
2.1 Division Minière de la Crouzille [8] [13].....	12
2.1.1 Geological Context [8] [13].....	13
2.1.2 Hydrogeological Context [13].....	14
2.1.3 Deposited Material [13].....	15
2.1.4 Climate Context [8] [13].....	17
2.1.5 Demographic Environment and Human	19
2.1.6 Water Usage.....	19
2.2 Industrial Mining Site of Bessines	20
2.2.1 History and Description of the Site [13]	20
2.2.2 Geographical Context [13] [16].....	21
2.2.3 Hydrographical Context [13] [16].....	25
2.2.4 Hydrogeology [16].....	27
2.2.5 Aftercare [10]	27
3. METHODOLOGY.....	30
3.1 Campaign and Sampling.....	30
3.1.1 Sampling by Piezometers	32
3.2 Laboratory Analyses	38
3.2.1 Chemical Laboratory of the Centre de Géoscience de Mines ParisTech.....	38
3.2.2 Chemical Laboratory of AREVA (Service d'Etudes de Procédés et Analyses) .	42

3.3	Simulation	43
3.3.1	Description of the Simulation Program HYTEC	43
3.3.2	Collecting of Data for the Simulation	44
4.	CHEMICAL COMPOSITION OF SURFACE AND GROUND WATER	47
4.1	Results of the On-Site Analyses	47
4.1.1	Results of the Laboratory of the Centre de Géoscience from Mines ParisTech	48
4.1.2	Results of the Laboratory of AREVA at the Industrial Site of Bessines.....	51
4.2	Piper-Diagram.....	52
4.3	HYTEC Simulation	54
4.3.1	Flow Rate	54
4.3.2	Evolution of the pH value	55
4.3.3	Sulfate	56
4.3.4	Muscovite dissolution and precipitation	57
4.3.5	Kaolinite dissolution and precipitation	58
4.3.6	Uranium Dioxide (Uranium (IV) Oxide).....	59
4.3.7	Detailed Examination of a Specific Point.....	60
5.	DISCUSSION AND CONCLUSION	62
5.1	Brief Review of the Aim and Structure	62
5.2	Discussion	62
6.	CATALOGS	64
	LIST OF REFERENCES	64
6.1	List of Abbreviations.....	66
6.2	List of Tables.....	67
6.3	List of Figures	68

1. Introduction

A significant uranium extraction activity took place in France between 1960 and 2000, particularly in the Limousin region. Limousin is located in the center of France and its landscape is mainly situated in the Massif Central. At the beginning of the 21st century the last uranium mine was closed.

Since then the local authority has to deal with a collection of closed sites. The main issues are acid mine drainage from waste rock piles, and the mobilization of hazardous chemicals from the tailings (here concentrated within the old open pit or underground mines). The monitoring and environmental management of these sites have been entrusted to AREVA.

The aim of the study is to improve the understanding of the hydrogeochemical behavior of the closed deposit in Bessines-sur-Gartempe. Bessines-sur-Gartempe is a village 35 km north of Limoges, the capital of the Limousin. Several piezometers have recently been completed on site for this purpose.

1.1 The Elements Uranium and Radium

Uranium is the 92nd-element in the periodic system of elements. It is part of the actinide group and a metal whose isotopes are all radioactive. It was discovered by the German pharmacist and professor in chemistry Martin Heinrich Klaproth in 1789 and named after the planet and Greek god Uranos. In fact, he only found a uranium oxide and the first isolation of the element was done in 1841 by the French Eugene-Melchior Peligot. 55 years later, in 1896, another French Henri Becquerel detected its radioactivity. The most common isotope is U-238, with a natural abundance more than 99%. [1]

Uranium is widely spread all over the world. Very small traces of this element can be found in rocks, the human body and natural mineral waters from the mountains. Obviously, uranium cannot be found in its native state but bound in minerals, chemical compounds with other elements. More than 200 different uranium minerals are known. [2] The mineral uraninite UO_2 , better known as pitchblende is one of the most intensive natural radioactive sources (157.8 kBq/g) and has a very high uranium content of 88.15 wt.-%. [3] The average concentration of uranium in the Earth's crust is 2 – 4 g per ton rocks, that means it is as common as tin and tungsten in the earth crust and more frequent than silver. [2]

Figure 1 shows the Uranium-Radium radioactive series. Most radioactive elements result from one of the three radioactive decay series: Uranium-Radium Series (beginning with U-238), Actinide Series (beginning with U-235) and Thorium Series (beginning with Th-232). Uranium 238 has, with about 4.5 billion years, a very long half-life. [4]

Uran – Radium – Reihe						Th-234	U-238
						24,1 d	4,5·10 ⁹ a
							Pa-234 1,2 m → h 6,7 h → 0,15 %
	Pb-214	Po-218	Rn-222	Ra-226	Th-230		U-234
	26,8 m	3,05 m	3,8 d	1600 a	8·10 ⁴ a		2,5·10 ⁵ a
	Tl-210	Bi-214	At-218				
	1,3 m	19,8 m	2 s				
Hg-206	Pb-210	Po-214	Rn-218				
8,1 m	22 a	162 μs	35 ms				
	Tl-206	Bi-210					
	4,3 m	5 d					
	Pb-206	Po-210					
	stabil	138 d					

Figure 1: Uranium-Radium Radioactive Series [4]

Radium is a decay product of uranium, which was first discovered in 1898 by Pierre and Marie Curie. They isolated it from pitchblende from North Bohemia in 1911. Radium is the 88th element of the periodic system and emits α , β and γ rays. Radium is an alkaline earth metal and over a million times more radioactive than the same mass of uranium. It is one of the rarest natural elements and every isotope is radioactive. [5]

1.2 Classification of uranium deposits [6]

The IAEA (International Atomic Energy Agency) based in Vienna, Austria, published a "Guidebook to Accompany IAEA Map: World Distribution of Uranium Deposits" in 1996. In this literature, several experts classified the existing uranium deposits worldwide.

"Uranium resources can be assigned on the basis of their geological setting to the following categories of uranium ore deposit types (arranged according to their approximate economic significance). [6]"

1. Unconformity related deposits
2. Sandstone deposits
3. Hematite breccia complex deposits
4. Quartz pebble conglomerate deposits
5. **Vein deposits (granite related deposits)**
6. Intrusive deposits
7. Volcanic and caldera related deposits
8. Metasomatite deposits
9. Surficial deposits
10. Collapse breccia pipe deposits
11. Phosphorite deposits
12. Other deposits

The deposit Bessines-sur-Gartempe belongs according to the IAEA classification to the “Vein type (granite related deposits)”. In Europe this type is very common in the Hercynian orogenic belt and range in age from Proterozoic to Tertiary. These deposits are associated with large batholiths of peraluminous leucogranite modified by late magmatic and/or autometamorphic processes. Uranium mineralization occurs within or in close proximity to a granitic intrusion. [6]” There are two different subtypes “based on their spatial relationship with granitic plutons and surrounding (intruded) host rocks: [6]” First, the Limousin-Vendée type, it is characterized as endo (or intra-)granitic deposits and related contact-granitic deposit; and second, perigranitic deposits in meta-sediments (monometallic Bohemian and polymetallic Erzgebirge types) and in contact-metamorphic rocks (Iberian type). As the name suggests of the deposit treated in this master thesis belongs of the Limousin-Vendée type. This type is described as “true veins and stockworks composed of ore and gangue minerals in granite, contact metamorphic rocks and in adjacent meta-sediments. [6]” It usually consists of “pitchblende and/or coffinite, which are commonly accompanied by gangue and alteration minerals. Deposits with simple paragenesis contain pitchblende in association with various amounts of pyrite/marcasite quartz, hematite, carbonate and minor base metal minerals. Complex deposits contain an important base metal sulfide stage (often with Co-Ni-As stage). In most cases, pitchblende is paragenetically early. The sizes of the vein and stockwork systems that characterize granite related deposits vary widely as to their configuration, size and complexity. [6]”

1.3 Uranium Mining worldwide

In 2012 58,394 tons of Uranium were produced. “64 % of the world’s production is from Kazakhstan (36.5 %), Canada (15 %) and Australia (12 %). After a decade of falling mine production to 1993, output of uranium has generally risen since then and now meets 86 % of demand for power generation. [7]”

“Mining methods have been changing. In 1990, 55 % of world production came from underground mines, but this shrunk dramatically to 1999, with 33 % then. From 2000 the new Canadian mines and Olympic Dam (largest known resource of uranium) increased it again. In situ leach (ISL or ISR) mining has been steadily increasing its share of the total, mainly due to Kazakhstan. [7]”

“Conventional mines have a mill where ore is crushed, ground and then leached with sulfuric acid to dissolve the uranium oxides. At a conventional mine or the treatment plant of an ISL operation, the uranium then separated by ion exchange before being dried and thereby precipitated. Finally it is packed usually as U_3O_8 . Some mills and ISL operations use carbonate leaching instead of sulfuric acid, depending on the ore-body. Where uranium is recovered as by-product, e.g. of copper or phosphate, the treatment process is likely to be more complex. [7]”

The world uranium production and demand is shown on Figure 2.

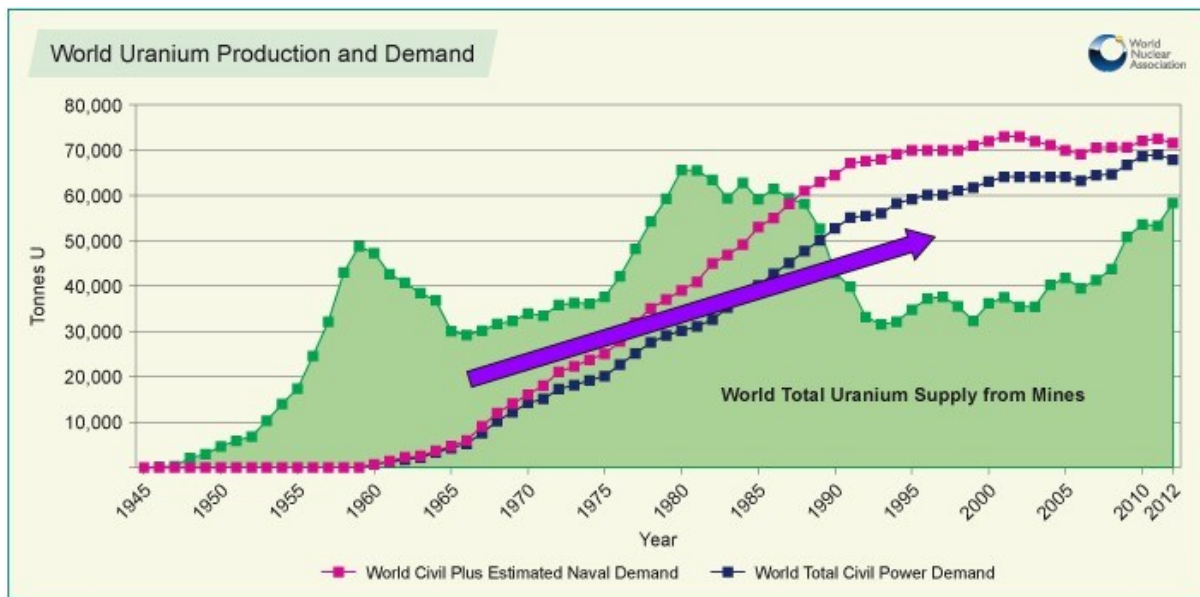


Figure 2: World uranium production and demand [7]

1.4 Legal Framework [8]

There are several European and national laws involved in the exploration, investigation, exploitation and aftercare of mining sites and especially uranium mining sites and their environment. In the European Union the Directive 2006/21/EC on the management of waste from extractive industries and the Directive 2000/60/EC EU Water Framework are of importance.

The national mining law in France is called “Code Minier”. It is pointed out by the general regulations of extractive industries (Règlement Général des Industries Extractives RGIE). Further important laws are the “code de l’environnement” especially environmental protection in the case of storage installations of the treatment residues and the “code de la santé” especially protection of the population of radiation phenomena.

The following paragraphs show the regulations for the different mining waste types: liquids, solids, uranium grit or other components, radon in the air and ambient gamma dose rate.

The French regulations are adapted to the recommendations of the International Commission on Radiological Protection (ICRP) which fixes the annual limits of incorporation by ingestion and inhalation for any radioactive element. These recommendations are most important for workers but are adopted for the public by dividing through a factor of 10.

The maximum permissible values for drinking water are shown in the following Table 1.

Table 1: Maximum permissible values of Ra-226 and U-238 for drinking water [8]

Ra-226	soluble	0.37 Bq/L	
	insoluble	1,110 Bq/L	
U-238	soluble	22,2 Bq/L	1.8 mg/L
	insoluble	1,480 Bq/L	

The ancient “Direction de la Prévention des Pollutions et des Risques (DPPR)”, which was divided in 2008 into the “Direction Générale de l’Energie et Climat (DGEC)” and the “Direction Générale de la Prévention des Risques (DGPR)”, created a circular of the January 29th 1986. It describes the regulations regarding the release of radioactive substances in the environment: definition of the point of release, limit values for short term, daily and monthly concentrations as well as daily freights. It helps to control the impact on the natural environment. Further it describes which aspects has to be controlled: release of dissolved species, water quality at the acceptor milieu, concentrations in fish, reeds, milk, herbs, potable water collector, ambient gamma dose rate and others.

The conditions of the mining division Crouzielle relate to prefectural orders pursuant to the decree Nr. 90-222 of March 9th 1990. This decree concretizes the general regulations of the extractive industries by the decree 80-331 of May 7th 1980 with the title “Ionization radiation” in respect of the environmental protection.

In article 6 it limits the acceptable annual exposure limit of the radiological impact to the environment:

- 5.0 mSv for external exposure
- 170 Bq for the alpha long-lived emitting radionuclide of U-238 present in the air as suspension and dust
- 2.0 mJ, the potential alpha energy for the daughter products of inhaled Radon-222
- 6.0 mJ, the potential alpha energy for the daughter products of inhaled Radon-220
- 3.0 kBq for the alpha long-lived emitting radionuclide of uranate dust (daily maximum 2.5 mg)
- 7.0 kBq for ingested radium
- 2.0 g for ingested uranium (daily maximum 150 mg)

The SI-derived unit Becquerel [Bq] of radioactivity is named after the researcher Henri Becquerel. A radioactive substance has an activity of one Becquerel. It describes nucleus decay per second: $1 \text{ Bq} = 1 \text{ s}^{-1}$

The specific activity is the number of the nucleus decay per second of 1g of a radioactive element or a pure chemical compound. The specific activity of ^{226}Ra is $3.7 \cdot 10^{13} \text{ Bq/kg}$ and of ^{238}U only $12.2 \cdot 10^6 \text{ Bq/kg}$.

The volumetric activity is activity per unit of volume; it is indicated as [Bq/m³] or [Bq/l].

Another SI-derived unit corresponding to the biological and health effects on human of radiation is Sievert [Sv]. This unit is named after the Swedish medical physicist Rolf Sievert and describes the equivalent radiation dose, effective dose and committed dose. It should not be mistaken with the SI-derived unit Gray [Gy] which describes absorbed dose of radiation energy (physical quantity). The units are both expressed as joules of absorbed ionizing energy per kilogram.

$$1 \text{ Gy} = 1 \text{ J/kg}$$

$$1 \text{ Sv} = 1 \text{ J/kg equivalent}$$

Referring to the radiation effect is the potential alpha energy concentration is very important. It is the sum of the potential alpha energy per volume of air. A common unit for this quantity is [J/m³]. This concentration is a very important factor concerning security in the mining industry because of the potential inhalation of alpha energy. The first correlation between lung cancer and radon gas was discovered in Schneeberg, Germany. The disease was called "Schneeberger Krankheit" (Schneeberg disease).

The decree further describes in article 8 the management of the solid radioactive products. The mineral and waste deposit has to consist a content of less than 0.03 % of lixiviated minerals; residues of minerals formed by treatment, products originating from the receiving water basin or its surroundings. The deposit should comply in accordance with a management plan for these wastes.

This content of uranium, 0.03 wt.-% corresponds to a specific activity of 3,700 Bq/kg of U-238. At this threshold the sedimented material in a natural milieu has to be excavated.

Article 9 describes the management of radioactive liquids. All exploitation waters (including runoff waters) have to be captured, observed and eventually treated. An insolubilization treatment is needed if the soluble radium has content higher than 3,700 Bq/m³. Between 740 Bq/m³ and 3,700 Bq/m³ are not an object of insolubilization treatments when the dilution factor is higher than 5. When the radium content is below 740 Bq/m³ treatment is necessary.

The corresponding circular letter of March 9th 1990 indicated in article 9, chapter III that the existing technology allows to limit the medium annual concentrations of radioactive substances to the following values shown in Table 2.

Table 2: Ra-226 and U-238 limits of the circular letter of the 9th march 1990 [8]

Ra-226	soluble	370 Bq/m ³
	insoluble	3,700 Bq/m ³
U-238	soluble	1,800 Bq/m ³

Finally the release limits are fixed for every site by prefectural orders supported by specific explanations. The industrial site Bessines sur Gartempe is under regulatory supervision. Several physical-chemical parameters are limited for discharge water.

1.5 Uranium Mining in France [9]

France has, similar to a lot of other European countries, a long history in mining. This tradition started in the French area in Neolithic era (5th to 3rd millennium BC) and stretched from the Celts and Gallic which exploited gold and tin (1st millennium BC). A big expansion took place in the Gallo-Roman period with the beginning of silver, lead, copper and iron exploitation.

After the fall of the Roman Empire all mining activities stopped until the beginning of the new millennium, however the next progress in mining in France took place during the industrial revolution (17th to 18th century AD). An independent industry, with technical innovations and a big diversification of exploited resources (oil, manganese, zinc and fluorite) was born.

The next evolution of the mining industry in France happened after World War II, France rebuilt the country and wanted to be self-sufficient with regard to energy supply

The exploitation of Uranium started after World War II and the last mine was closed down in 2001. Figure 3 shows the exploitation areas in France. The decline of other mining sites started also at the end of the second half of the 20th century. Nowadays only some salt quarries are still operating.

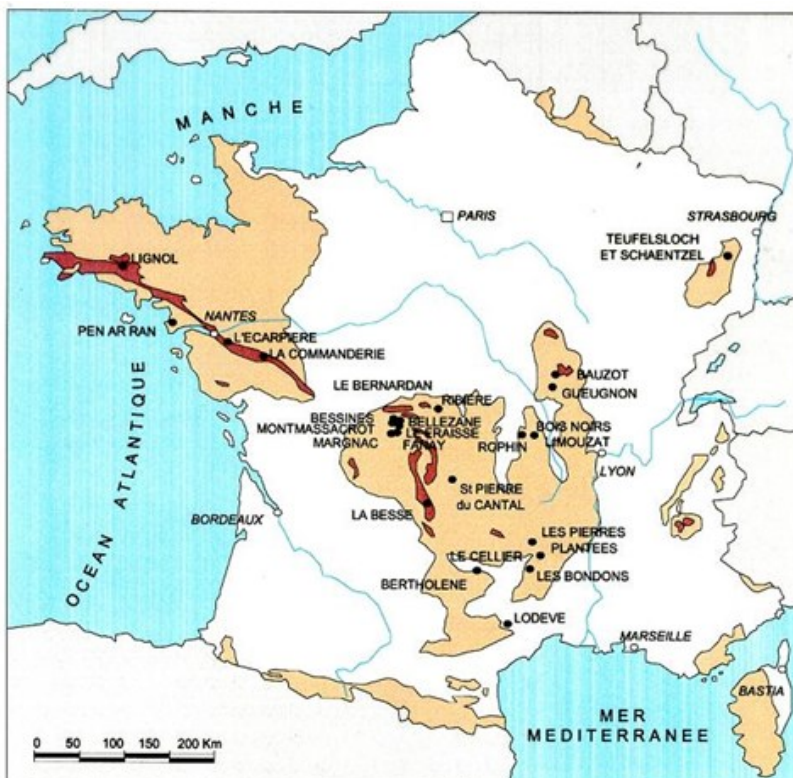


Figure 3: Uranium exploitation in France [10]

1.6 Uranium Mining in Germany [11]

Mining in Germany has a 4,500 years old history. It started with the digging of copper. At the beginning only native metals were recovered i.e. copper, silver, gold. In the Bronze Age the first weapons of bronze, an alloy of tin and copper were developed. In the Middle Age mining in Germany furnished. The ore mining lasted at least several hundred years but with the beginning of the 20th century the last mining sites closed due to economic reasons.

1.6.1 Uranium Mining in Schlema-Alberode [12]

1.6.1.1 Introduction

The first mining activities in this area were Ag und Co mining in Schneeberg, as well as some uranium sporadic co-product since 1797. A detailed investigation of Oberschlema started since 1905 because of radioactive signs in surface and mine water. These radioactive waters are the basis for the growth of Oberschlema as a radium spring with a world reputation. During investigation work for new water inlets in 1929 uranium ores were found without a direct conclusion to pitchblende ores.

The uranium deposit in Schlema-Alberode is in the federal state of Saxony, Germany, close to the Czech border. It was discovered after the World War II by Russian geologists. This deposit is one of the biggest uranium deposits of this vein type in the world. The extraction by WISMUT GmbH started in 1946 and ended in 1991, and produced about 8,000 metric tons of uranium. The deposit was extracted almost completely, except some small reserves. This work was accompanied by extensive and detailed exploitation work and scientific investigation. In 1991 the aftercare works started and took about 20 years.

The deposit is part of the ore field Schneeberg-Schlema-Alberode in the NW border area of the Hercynian fold- and thrust-belts of the Bohemian Massif. In this area is the reservoir at the northern descents of the ore mountain pluton granitoid and the intersection of two tectonic major structures: Lössnitz-Zwönitzer-basin and Gera-Jáchymov-fault-zone.

Almost 80 % of the uranium storage was between -200 m and -800 m, and 20 % in the areas 0 m-200 m and 800 m-1000 m. In 200 m-800 m the rocks were of "productive series" inside the aureole.

General Information

The annual average temperature in this area is 13 °C and the annual precipitation about 810 mm. This area is intensily populated and characterized by an enclosed urban area between Aue and Schneeberg within 40,000 inhabitants.

The area is drained by the Zwickauer Mulde (into the Zwickau basin). The Zwickauer Mulde has in Niederschlema an average discharge of 11 m³/s, among which the Schlemabach is the largest with 0.3 m³/s. The afflux is, in general, discontinuous and strongly influenced by

meteorological conditions. In this area efficient aquifers are missing, so heavy rainfall and snowmelt causing rapid discharge by the before called drainages systems.

Remedial Action

The remedial actions are mentioned by the office Aue of the WISMUT GmbH and other contracted companies. The reclamation concept contains following design states:

- Keeping the mine plant
- Flooding the mine including disposal of compounds hazardous to water
- Treatment/preparation of contaminated mine water and dump seepage water
- Deconstruction of industrial installations as well as remedial action and reclamation of factory spaces
- Keeping and reclamation of stock piles
- Keeping of the sedimentation plant

Depression ventilation allows for directed radon deduction by an outlying air stack. The uranium concentration of the waste tips contains less than 100 mg/kg, the radium activity between 0.3 Bq/g up to 5.0 Bq/g and the arsenic concentration contains between 100 mg/kg and 300 mg/kg.

The flood water contains concentrations of uranium, radium, arsenic, manganese and iron. A direct discharge release 35 t uranium and $21 \cdot 10^9$ Bq Ra-226. The other elements would require an addition burden in the same order as the present geogenic contamination. The water treatment plants do a selective precipitation of these harmful substances. The effluent limits are 0.5 mg/l uranium, 0.4 Bq/l Ra-226, 0.1 mg/l-0.3 mg/l arsenic, 3.0 mg/l manganese and 2.0 mg/l total iron. The leachate contents as well uranium, radium and arsenic but only the last one occurs in high concentrations (> boundary value) which results in passive treatment plants with application of reactive substances.

2. The Uranium Deposit Bessines-sur-Gartempe

This chapter gives an overview of the different factors that influence the area around the industrial site Bessines-sur-Gartempe. Beginning with the former mining division where this site is part of it and then continuing with a more detailed description of the site.

2.1 Division Minière de la Crouzille [8] [13]

The mining site in Bessines-sur-Gartempe belongs to the old division Crouzille (Division minière de la Crouzille), the oldest uranium mining area in France. This division of 800 hectares was exploited from 1948 to 1995 by open pit mining for the resources close to the surface and by underground mining for the deep-seated deposits. In this division 24,000 tons of uranium were exploited between 1950 and 1995.

- The concession of Lacour: one mining site
- The concession of Lavaud: one mining site
- The concession of St. Sylvestre: twelve mining sites
- The concession of Gartempe: ten mining sites, including Bessines-sur-Gartempe

Figure 4 shows the localization of the site “Bessines-sur-Gartempe” in the Crouzille Division. Between 1958 and 1993 the extraction of the minerals was conducted at the industrial site of Bessines. The excavated material (13.7 million tons of the dynamic treatment and 8.7 million tons of the static treatment) was stocked as backfilling material for the closed down open pit sites or as dikes of the basins for the process and surface water.

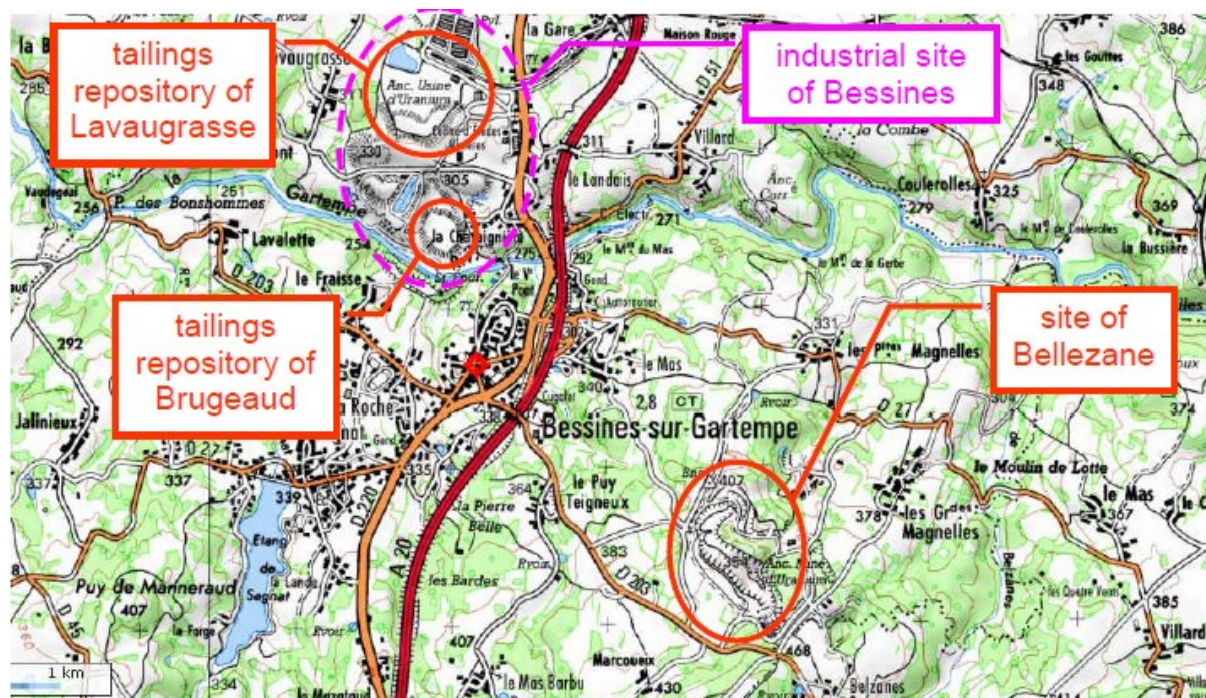


Figure 4: Localization of the sites inside the Crouzille Division [14]

In these 800 hectares are several watersheds, the most important are:

- River Gartempe (9 sites)
- River Vincou (2 sites)
- River Ritord (5 sites)
- River Couze (4 sites)

Certainly the rivers Couze, Ritord and Vincou are affluents at the left side of the river Gartempe. Other watersheds in this area are the rivers Brême (1 site), Semme (1 site) and Vienne (2 sites).

The mining area next to the Gartempe constitutes therefore a source of radioactivity which doesn't correspond to the baseline condition of the environment before exploiting the raw materials.

2.1.1 Geological Context [8] [13]

The region Bessines is situated in the northwest of the Massif Central, in the leucogranite in the Ambazac Mountains. This intragranitic massif consists of three units which are located on an east-west axis:

- In the west, the biotite and sillimanite granite of Brême intersected by fine-grained two-mica and andalusite granite called "Chateau ponsac",
- In the east, muscovite granite of Saint Goussad,
- In the center, the muscovite and biotite granite of Saint Sylvestre which has a locally porphyritic tendency and is intersected by fine-grained biotite called "Fanayain" or muscovite called "Sagnes".

The Saint Sylvestre granite can also be characterized by the presence of:

- Lamprophyres (minettes): These veins strike in the north-north-east with a dip angle of 75 ° into the west and with thickness ranging of 0.5 to 10 meters. They have a microgranular texture and consist of feldspar, biotite, augite and geological old olivine.
- Microgranite: These veins are not frequent but very thick; they have the same strike and dip as the Lamprophyres with whom they are associated. They have a phenocrystalline texture and consist of biotites and plagioclases.
- Episyenite: This rock is a result of the locale dequartzification of granite. There are two types: the dense feldspathic episyenite and the porous micatic episyenite (30 % of the void volume). These last types are in the form of columnar agglomerations at the junction of systems of faults and joints.

The granitic rock is affected by different tectonic episodes:

- Fractures into the north-east with a dip of 75 ° to the west
- Fractures into the east-west with a dip of 75 ° to the north

The average geochemical backgrounds of uranium of this bordering granite are some dozens ppm and locally up to 100 ppm. The principal mineralization is uraninite which is a radioactive mineral with a chemical composition that is generally UO_2 , but also covers UO_3 and oxides of lead, thorium and rare earth elements. It is usually known as pitchblende. The lamprophyres are often the main area of mineralization favored by the intersection of the faults lancing the massif.

The mineralogical composition of the tailings consist of 90 to 95% of primary minerals (i.e. from the host rock), about 5 % gypsum and 1 % to 2 % of carbonates (resulting both from sulfuric attack and from the neutralization), and finally of iron oxides (2 % to 10 %), and other metal oxides (up to 1 %). [15]

2.1.2 Hydrogeological Context [13]

Granite is a hard and compact rock. At the surface area it weathers to grus. This is a granular mixture of quartz, clay and lower weathered minerals. This process of alteration is favored where water circulation through granite fissures is close to the surface. The thickness of grus increases at the valley end and is porous in the center which contains a discontinues aquifer which serves with a break-out the small collected sources of the becks.

In granite water prefers the fracture network for circulation. These fractures band together and give an area-wide permeability but the porosity stays low. The water flow in the granite is large but its water storage capacity is low.

In this environment the piezometric surface follows the topography. This level appears at the source level at the transition of granite and grus or fractures and its cutting point with the topographic surface.

In the Saint Syvestre granite water flows through the joint and continues via lamprophyric veins (between 0 m and 50 m depth) as drain.

The permeabilities of the different rock types can be found in Table 3.

Table 3: Permeability of the different types of granit [13]

Terrain	Permeability [m/s]
granitic sand	$10^{-6} - 10^{-4}$
granite	$10^{-9} - 5*10^{-4}$
fractured granites because of mining operations	$7*10^{-7} - 5*10^{-5}$

2.1.3 Deposited Material [13]

2.1.3.1 Mine Tailings

The exploitation of uranium ore deposits has led to the production of two types of mine wastes:

Barren rock: Gangue material is extracted to access the deposits. In this context they are uraniumiferous granites of the Limousin. The uranium concentrations of these materials are between 10 ppm and 100 ppm (average 17 ppm to 24 ppm).

Low-grade ore: can be found in the aureole or inside the repository, it is common to find rocks with content a higher concentration of uranium than barren rocks but below the cut-off defined by the criteria of relevance.

Before 1991, the cut-off grade was 200 ppm for material to be conveyed from underground mining and 100 ppm from open pit mining. From 1991 on, the cut-off increased up to 400 ppm for economic reasons.

The low-grade ore has an average grade lower than 150 ppm.

All mine tailings were deposited close to the extraction site except materials with content of more than 300 ppm; they are used as backfilling material for open pit mining sites (pursuant to Order No. 90-222 of March 9th 1990).

2.1.3.2 Treatment Residues

The ores were treated by two methods according to their uranium content:

Static leaching treatment for low-grade ores (100 ppm–600 ppm uranium),

Dynamic leaching treatment for higher-grade ores (> 600 ppm uranium).

Static or heap leaching treatment: the ore (raw or cracked) is sprinkled by sulfuric acid which yields the extraction of 60 %-80 % of all present uranium. The residual concentration of uranium is 60 ppm.

These residues of heap leaching are used as materials for the first coverage over the residues of the dynamic treatment of the storage of Brugeaud and Lavaugrasse or covered with barren material.

Dynamic leaching treatment: First they were transported to the processing plant where they were crushed and grounded mechanically. Then they were processed and purified with certain chemical solutions. Next step was extracting from the resulting liquor organic solutions or ion exchange resins. At last the material was washed, filtered, precipitated and dried.

They are sandy clay (mean particle size < 450 µm) with the same mineralogical composition as the original ore plus chemical precipitates. These residues essentially contain the radionuclides (^{238}U , ^{235}U and ^{226}Ra) including radium very insoluble in almost all the solid residue. The residues of the dynamic treatment contain both primary minerals from the deposit and newly formed minerals from the treatment: Primary minerals are quartz fragments, feldspar, mica and intensely weathered sulfides. Secondary minerals are gypsum oxy-hydroxides of iron and clay minerals (as cement around primary minerals and is formed after the deposition of residues)

The chemical composition of dynamic treatment residues is presented in Table 4.

Table 4: Results of the analysis of the solid residues of the dynamic treatment [13]

Solid	Mass Proportion
Silica	50-70 %
Alumina	10-16 %
Iron Oxides	2-10 %
Sulfates	5-8 %
Calcium Oxide	3-6 %
Other Oxides	1 %
Uranium	100 g/t
Radium	0,0006 g/t

After the dynamic treatment the residue were subjected to tailing management processes: One part of the residues underwent a size separation by cyclone into two fractions:

A coarse fraction (0.15 mm to 0.50 mm) composed of sands with residual minerals resistant to chemical attack; the primary minerals originated from the local uraniumiferous granites and keep their composition during the treatment. This sand is used in backfilling and underground mining sites for the constitution of the dikes of Brugeaud and Lavaugrasse.

A fine fraction (<0.15 mm) consists mainly of clay minerals impregnated with sulfates and hydroxides generated by the treatment. It is stored with those residues which have not been classified by a cyclone in open pit mining sites or the supply basin.

The ranges of permeabilities of the stored materials are presented at Table 5 as ranges of permeability of the backfilling material.

Table 5: Ranges of permeability of the backfilling material [13]

Material	Permeability (m/s)
Non compacted barren material	$10^{-7} - 10^{-6}$
Compacted barren material	$2.8 \cdot 10^{-7}$
Treatment residue	10^{-8}

2.1.4 Climate Context [8] [13]

All the plateaus in the west of Limousin have an oceanic climate and are influenced by the Atlantic Ocean. This climate is characterized by:

- An attenuation of weather conditions
- Even precipitation during the year with seasonal turnovers
- A predominance of rain in fall and in winter
- Long-lasting rain but few heavy raining events

2.1.4.1 Precipitation

The precipitation of Haute Vienne is strong at higher elevations. The average rainfall is about 1000 mm per year. The average rainfall at the mining area is between 900 mm (North of the ancient Divison Minière) and 1200 (Sector St. Sylvestre) at which the gauging station in Bessines-sur-Gartempe measures an average rainfall of 1000 mm (Figure 5). Figure 6 shows a significant rainfall throughout the year and even the driest months of the year have still a lot of precipitation. The difference between months with low precipitation and months with high precipitation is in the middle 30 mm.

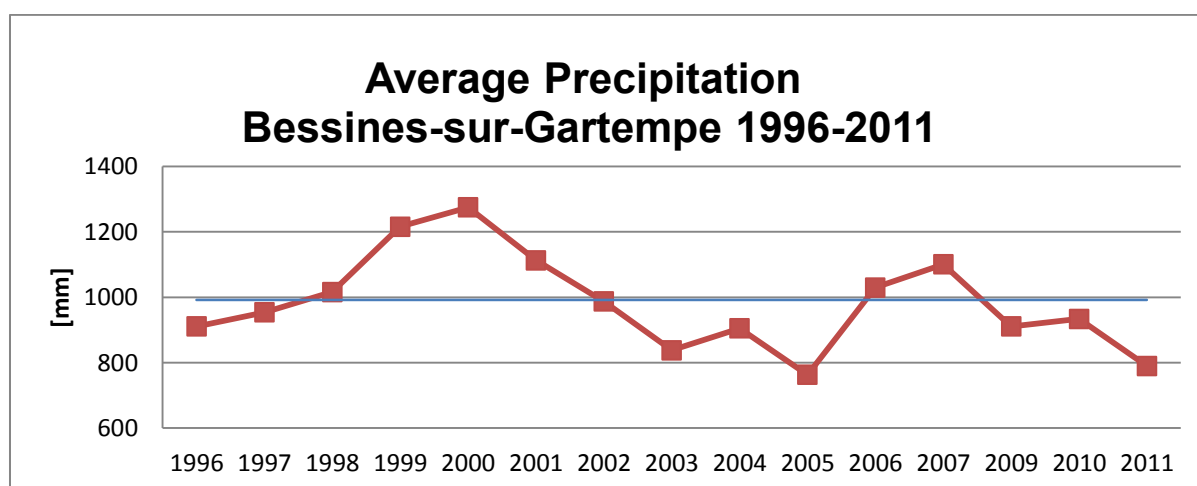


Figure 5: Average rainfall Bessines-sur-Gartempe 1996-2011 [8]

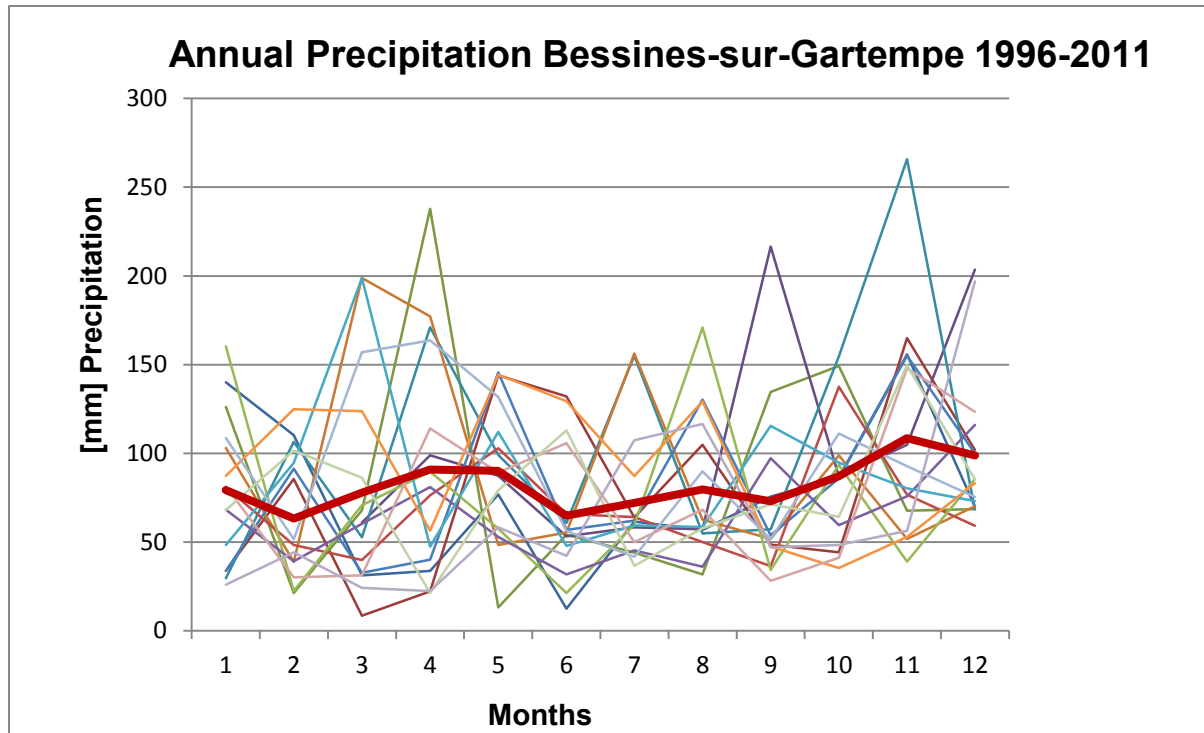


Figure 6: Annual rainfall Bessines-sur-Gartempe 1996-2011 [8]

2.1.4.2 Temperature

The decoding of the thermal curves shows the same constitution as the rainfall curves. The temperature decreases towards the direction of the basin of the river Gartempe. The average temperatures of the last 30 years (1969-1998) of the gauge station in Bessines-sur-Gartempe are shown in Table 6. The Table 6 shows that the region Limousin has a temperate climate. The average temperatures vary during the year by 10.6°C.

Table 6: Average temperature (°C) in Bessines-sur-Gartempe [8]

Month	Average Monthly	Minium Monthly	Maximum Monthly
January	3.9	-2.2	7.6
February	4.6	0.9	9.2
March	6.7	2.6	9.8
April	8.8	6.2	11.8
May	13.0	9.9	15.7
June	16.0	13.6	18.8
July	18.5	15.5	23.2
August	18.2	15.6	21.6
September	15.0	12.3	17.8
October	11.4	6.4	15.3
November	6.8	3.5	10.5
December	4.6	0.7	7.3
Year	10.6	9.2	12.4

2.1.4.3 Wind

The dominant winds come from the south-west and north-east. At rare intervals are the winds which descend from the east or the south-east.

2.1.5 Demographic Environment and Human

The territory of the ancient Division Minière de la Crouzielle has a population of 8500 inhabitants. It has a rural character with some villages. The villages Bessines-sur-Gartempe, Razès, Compreignac, Bersac-sur-Rivalier and Saint Sylvestre are as important to have a public primary school. Only Bourg-de-Bessines is as important for a public secondary school.

A complete investigation of all living areas in a radius of 1 km around the sites identified 93 populated areas which can be influenced by the closed down mining sites.

2.1.6 Water Usage

In Haute Vienne the most communities are autonomous and get their potable water from high ground water tables. Lots of the communities of the Gartempe and Couze Valley (Bessines sur Gartempe, Folles, Razès, St. Pardoux) are grouped in the Syndicat Intercommunal d'Adduction d'Eau Potable Couze-Gartempe (Intercommunal household drinking water supply) which is managed by Lyonnaise des Eaux.

The only water-associated leisure activities practiced at the border of the Gartempe is fishing.

2.2 Industrial Mining Site of Bessines

2.2.1 History and Description of the Site [13]

This industrial site is as already mentioned part of the old mining division Crouzielle. The exploitation started in 1955 with an underground mining situated in Brugeaud. The exploitation of the deposits was in progress until 1967. The levels were between 54.4 m and 270 m NGF (Nivellement général de la France).



Figure 7: Open pit mining site of Brugeaud in 1955 [10]

The open pit mining in Brugeaud started in 1955 (Figure 7). The initial ground of the mine was 225 m NGF that is 65 m deep, and has been extended to 170 m NGF after the redirection of Gartempe between 1962 and 1964. The open pit mining was closed down in 1978 and caused 14 million tons of the material.

The deposit of the residue started in 1960. The natural basin of Lavaugrasse was used for deposition after building a dam composed of barren material and sand fraction of the treatment residues. The construction of the dam continued to progressively filling until 1987. In total numbers 5.678 million tons of residues were deposited at the basin of Lavaugrasse.

From 1978 to 1987, the storage continued of residuals in the open pit mining site Brugeaud, whose capacity has been increased by building a dam in the southern portion in 1982. It was built by and by using the sand fraction of rejection.

In 1992, the basin of Brugeaud was above the water level to allow the establishment of toe drains of the dike to capture upwelling water. The pumping was situated at the former mining pit P2, at its former relative elevation of 250 m NGF. The pumping was stopped at the end of 1998.

In the years 1993 to 1995 was the treatment plant closed, and the products of dismantling have been stored in the pit Jean-Jeanette, located north of the basin Brugeaud.

From 1995 to 1999, redevelopment was undertaken at the sites Brugeaud and Lavaugrassse. A cover and dams were constructed on the basin of the barren materials and dams. To improve the system of water harvesting and to close the gap between the dam of Lavaugrassse and the waste dump in the south, they filled all with barren material.

Finally, between 2003 and 2006, the recovery of the storage area Jean Jeanette was made.

2.2.2 Geographical Context [13] [16]

The industrial site of Bessines is situated on the north side of the valley of the river Gartempe, close to the municipality Bessines-sur-Gartempe in the department of Haute-Vienne (87). It is limited in the north through D 711 (route départementale; county road), in the south by Gartempe and in the west by a place called Lavaugrassse and in the east by the D220. The site has an area of 140 ha and contains two disposals of residues: the open pit mining of Brugeaud and the basin of Lavaugrassse. The area includes also a district with offices, laboratories and storage for the depleted uranium-oxide. You can see all this different areas of Bessines in the Figure 8.

The borders of the study area are:

- In the south the river Gartempe
- In the east the thalweg of Vaugoudreix
- In the west with a thalweg in between Bois-du-Mont and Lavaugrassse
- In the north by a topographic crest which follows the route D 711



Figure 8: Area of the Industrial Site of Bessines

2.2.2.1 Description of the Mining Operations and Storages [16]

Open Pit Mining at the Sector Brugeaud

The open pit mining site of Brugeaud has an ovoid form. It measures 500 m in the north-south axis and 250 m in the east-west axis. The mining site has a depth of 120 m referring to the actual level of 297 m NGF. It has a step-line of 10 m latitude and 10 m height. The

exploitation took place from 1957 to 1972 after closing-down as a mining pit it was used as residue storage from 1978 to 1987.

Underground Mining Brugeaud

Today, the underground mining of Brugeaud includes:

- The vertical descent partially stocked and equipped with monitoring wells. Little information exists of this characteristic plant. The wells have an estimated depth of 50 m and a diameter of 30 cm at the head. The casing is limited by a former rockslide in 1992 to forty meters. This work was used between January 1992 and December 1998 to realize a pump which allows holding the water level at elevation 250 m NGF so as in order to run dry the exudations at the foot of the dike till drainage was made.
- The pseudo-horizontal galleries are also partial stocked and/or blocked by a cement plug, sometimes it drains in the open pit mining site.
- Two joining tunnels between the vertical descent and the underground mining site of Vieux Moulin at a level of 60 m and 125 m. They are an obstruction drainage aiming a disconnection from Brugeaud and Vieux Moulin.

Underground Mining Site Vieux Moulin

Vieux Moulin constructed basically an underground mining site with different driving sectors and a small open pit mining site with a depth of about thirty meters. After partial depression and leveling nothing is left of this open pit mining. Today the underground mining of Vieux Moulin is arranged as:

- Sub-horizontals galleries
- Refilled driving sectors with fine fraction
- A security exit gallery which has a drainage system to the basin of Vieux Moulin. There can be conducted different analytic measurements.

Storage and Stock Pile

At the closed down industrial mining site of Bessines there are two storage basins of the mineral and industrial residues:

- The basin of Lavaugrasse was a natural depression with an ancient thalweg. This basin was used as treatment residue storage from 1958 to 1978. In the south it is enfolded by a dike which ranges from the east to the west. The dike consists of mine and barren material. The basin measures 500 m by 700 m and achieves a mightiness of 10 m to 60 m.
- The open pit mining site Brugeaud has collected the treatment residues since the end of exploitation (1978 to 1987). The mightiness of the storages is between 10 m and 120 m. Two dikes one upon another hold off the stock drain outlet. The first dike covers the ancient river bed of Gartempe (redirection to the south). This dike, so-called thalweg, has a clay core and is underlain by granite. The other dike extends

from the edge of the dike of the thalweg to a height of 290 m NGF. The second dike consists of cycloned sand deposited by backward scheduling.

There are also two waste tips:

- The “waste tip west” between Lavaugrassse and Vieux Moulin can reach a mightiness of fifty meters and consists of leaching residues and is covered by barren material.
- The “waste tip Aupuybertrot” in the north of Brugeaud and the route of Lavaugrassse consists of static leaching residues and the mightiness is between fourteen and twenty meters in the center.

Table 7 shows data of the named storages and waste tips.

Table 7: storage and stock pile data [13]

Stock	Max. Depth	L x W	Content	Amount
	m	m		tons
Brugeaud	120	500 x 290	Static and dynamic treatment residues of site industriel de Bessines (min. 99%), industrial plant Bouchet and drums from Pierrelatte	5,760,000
Lavaugrassse	60	500 x 700	Static and dynamic treatment residues of the industrial site Bessines (min. 99%) and industrial plant Bouchet	5, 678,000
Ancient open-pit of Vieux Moulin	30	100 x 100	Goaf (effondrement)	0.0
Waste tip west	50	400 x 350	Static treatment residues of the industrial site Bessines	1,806,000
Waste tip Aupuybertrot	20	400 x 200		unknown

2.2.3 Hydrographical Context [13] [16]

2.2.3.1 Present Situation

The area of Bessines is situated in the drainage basin of Gartempe. It is mainly drained by the river of the same name, which runs at an average rate of $8.2 \text{ m}^3/\text{s}$ ($690,000 \text{ m}^3/\text{y}$). The river coast of Gartempe is about 260 m NGF upstream and 250 m NGF downstream. The bed of the river was diverted to the south during exploitation of the mining site, requiring the excavation of $410,000 \text{ m}^3$ materials and the establishment of three clay core dikes. This work was carried out in June 1962 and July 1964.

The site contains steep slopes, resulting in heavy runoff. A network of drains was set up and allows effluent control. Subsurface flows occur within the granite cracks. Due to the topography of the site, runoff is predominant on the refill.

Gartempe has three feeders which flow from the north to the south. One flows to Gartempe at the height of the industrial site Bessines and the two others downstream.

A source is in the north-east of the village Lavaugrasse, in the thalweg separating the village of the site with the same name. It has a flow rate of $3.1 \text{ m}^3/\text{y}$ (measured August 17th 2011 of Burgeap). This source feeds a stream which flows to the south and flows to the river Gartempe.

It has been observed that the water infiltrates the river Gartempe from the granite, especially at the right side of the storage of Brugeaud.

2.2.3.2 Situation before the start of mining

The topographic map (Figure 9), from the time before the exploitation started, shows old runways in the granite with a north-south orientation. The map presents a fibered hydrographic system with a drainage channel to the ancient bed of the Gartempe (light blue line at Figure 9).

The storage basin of Lavaugrasse was realized during the construction of one dike crossing this valley. These structures are today covered with deposited materials (dike, residues, waste tips) creating the axis of the drainage system which collects the most waters in the zone of Lavaugrasse percolating through the waste tips of Vieux Moulin. These waters accentuate downstream to the site at the points SIBDOB and SIBDOB2.

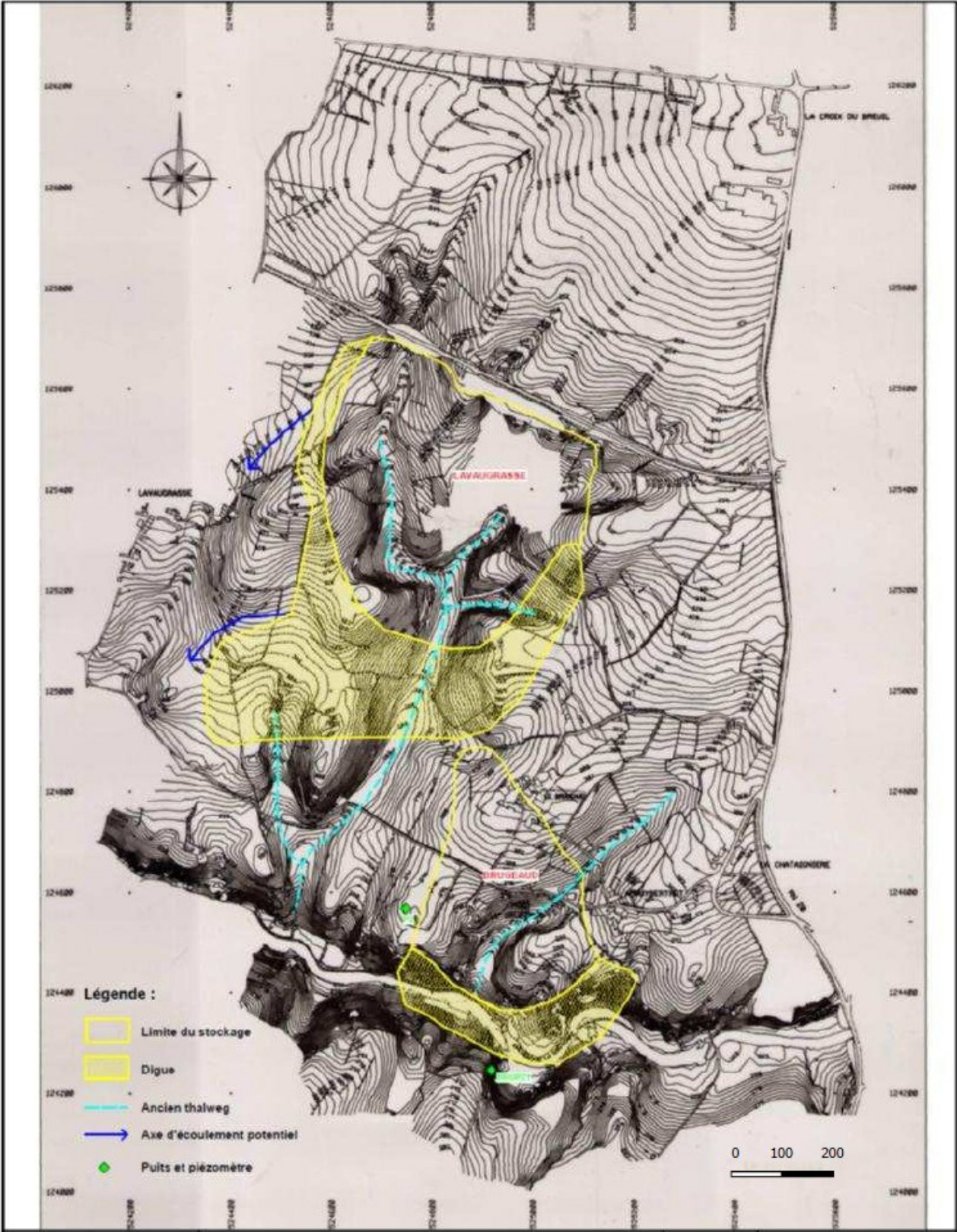


Figure 9: Ancient hydrographic network [13]

2.2.4 Hydrogeology [16]

At the industrial site of Bessines there are three different hydrogeological units:

- The granitic basement, where the groundwater flows along a network of fractures. This fractured granite has a variant transmissivity and bad groundwater storage.
- The covering materials are constituted by granitic sand which issues a break-up of the subjacent stones. The mightiness of this bed varies between some centimeters and twenty meters. The importance of this aquifer of granitic sand is limited by the bad extensiveness of this repository. This aquifer is characterized by a moderate transmissivity and important groundwater storage.
- The anthropogenic deposition stored at the basin of Lavaugrasse and at the open pit Brugeaud has small local reservoirs and a bad permeability.

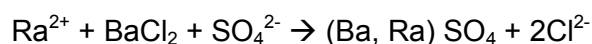
2.2.4.1 Water Collection and Treatment [15]

In general there are four different water types at mining sites:

- Total collection of all transitional waters trough the ancient open pit mining sites and waters flowing through the drainage system of the massif
- Total collection of waters passing the surface of ancient mining areas (no flooded areas)
- Partial collection of waters at the foot of the waste tips
- Non collection of the waters which escape the drainage system

Physical-chemical water treatment for all waters at all mining sites were done from 1977 to 1994. Beginning in 1994 research work was done to improve the water treatment methods.

The common method for elimination of radium is a chemical precipitation by adding barium-chlorite ($10\text{-}50\text{ g/m}^3$) in the presence of sulfate ions:



Removal of uranium also works by chemical precipitation by adding aluminum-sulfate ($\text{Al}_2(\text{SO}_4)_3$) or ferrous chlorosulfate (FeClSO_4 $25\text{ g/m}^3\text{-}170\text{ g/m}^3$) and setting the pH-value with natron (NaHCO_3).

A flocculation medium (iron(III) chloride or organic flocculation medium; $40\text{ g/m}^3\text{-}60\text{ g/m}^3$) helps by clarification of the waters.

These methods reduce up to 70 % of uranium and up to 90 % of radium.

2.2.5 Aftercare [10]

The cultivation of a closed down mining site covers several steps. Figure 12 shows the mining site Bessines-sur-Gartempe in 1978 before the recultivation works started and Figure 13 shows the industrial site reshaped in 2001.

- Detailed survey
- Project for redevelopment
- Dismantling
- Safety requests
- Sanitation
- Redesigning and civil engineering
- Revegetation

For open pit mining sites different procedures are needed than for an underground mine. For open pit mining sites a redesigning was done with a back filling, a management of the water reserves and a vegetable reinforcement. The underground mining sites need besides a reshape and revegetation also physical safeguarding measures between the connection paths of the underground and surface as well as measurements to prevent depressions.

The natural depression Lavaugrasse was totally refilled with residues of the treatment and supported by a ring dike (Figure 10).

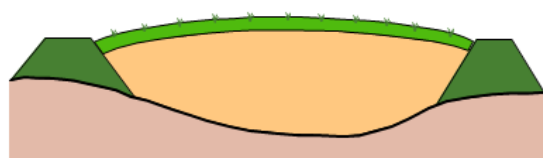


Figure 10: symbol icon of Lavaugrasse [10]

The aftercare includes not only water treatment and surveillance at the ancient mining site but also investigation of the atmosphere, the vegetation and water milieu of the environment (water, sediments, flora and fauna) including underground water. Figure 11 shows the hedging of the storage of residues. The different layers provide as mechanical and radiological protection.

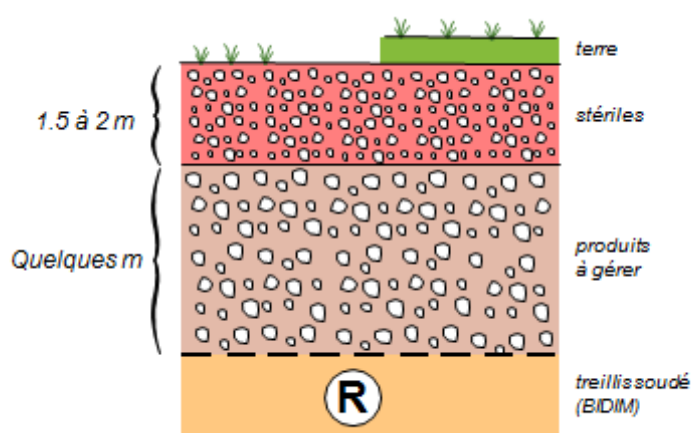


Figure 11: shows the hedging of the storage of residues. The different layers provide as mechanical and radiological protection. Figure 11 Reinforcement of dikes, hedging (First layer... Residues with a welded wire mesh, second layer ... protection structure against radioactive transports, third layer ... barren rock) [10]



Figure 12: Mining Site Bessines-sur-Gartempe in 1978 (TMS... underground mining; MCO... open pit mining) [10]



Figure 13: Mining Site Bessines-sur-Gartempe after reclamation in 2001 [10]

3. Methodology

The first task is to acquire the basic hydrogeological parameters, well testing for permeability and amount of water easily available. The analyses of historical and hydrogeological data should help pinpoint the critical points for water analysis (up to downstream from the tailings, outlet from the old underground mine).

The study involves water sampling and analyses of basic geochemical field parameters (temperature, pH value, Eh value, alkalinity, conductimetry), which will give a first idea of the history of these waters. The samples are analyzed for major elements and metals. Uranium and radium will be analyzed by a specialized laboratory of AREVA.

These data are used to build up a conceptual hydrogeochemical model of the site. The simulation will be performed with the program HYTEC, a program developed by engineers of Mines ParisTech. With this model a quantitative evaluation of the water fluxes and chemical reactions within the site and long term behavior of the pollutant release from the site can be achieved.

3.1 Campaign and Sampling

From 25th – 27th April 2012, a field campaign including an in-situ determination of the groundwater level and hydrogeochemical parameters of surface and groundwater took place at the Site industriel de Bessines (Figure 14, Figure 15). Groundwater sampling (PZ94 – PZ98) was conducted by piezometers (Figure 16), whereas sampling of surface water, at selected wells (SIMOGAL, SIBDOB, SIBDOB2) was conducted by sampling vessels.

During the time of the samplings and in the days before, it has been raining a lot in this area.

At all-sampling sites two samples were taken, one for the laboratory of the Centre de Géoscience and one for the laboratory of AREVA. The examination of radioactive components was made in the laboratory of AREVA which has the relevant equipment.



Figure 14: Location and numeration of measurement and sampling sites



Figure 15: Look at the basin Vieux Moulin [16]

3.1.1 Sampling by Piezometers

The sampling started with measuring the water level with an electric water level gauge. It is a precise and quick method.

The next step was pumping the ground water with the water pump MP1 from Grundfos. This pump is designed for pumping cold groundwater. The pump should be completely submerged at all times during operation. The maximum rate is 34.07 liters per minute (max. 9 gallons per minute) and the motor is a 3 phase 220 VAC with 400 Hz. To obtain a representative sample the entire standing water has to be removed from the well and a pumping rate has to be chosen, with which the ground water level can be maintained.



Figure 16: the equipment for the pump MP1 and the pump MP1 [17]

Figure 16 shows the pump MP1 connected to a pipe and is operated by a generator.

The figures (Figure 17, Figure 18, Figure 19 and Figure 20) on the following pages show the depth profiles of the measured piezometers. PZ98 and PZ95 (Figure 17 and Figure 18) have both a similar depth of 57.85 m and 56.00 m. Their profile also starts with a granitic fill-up. PZ98 has only 5 m digging and PZ95 a charge of 23 m. The main layer of PZ98 comprise 40 m sandy clay and of PZ95 30 m granite. In contrast the piezometers PZ96/96B and PZ94 (Figure 19 and Figure 20) have also a similar depth but only 20.20 m or 20.40 m. The first layer is grus but also in different mightiness. The main layers are at both cases about 10 m altered granite and fractured granite.

GINGER
CEBTP

SONDAGE CAROTTE LVG1

Chantier : Sondages carotés

Client : AREVA NC

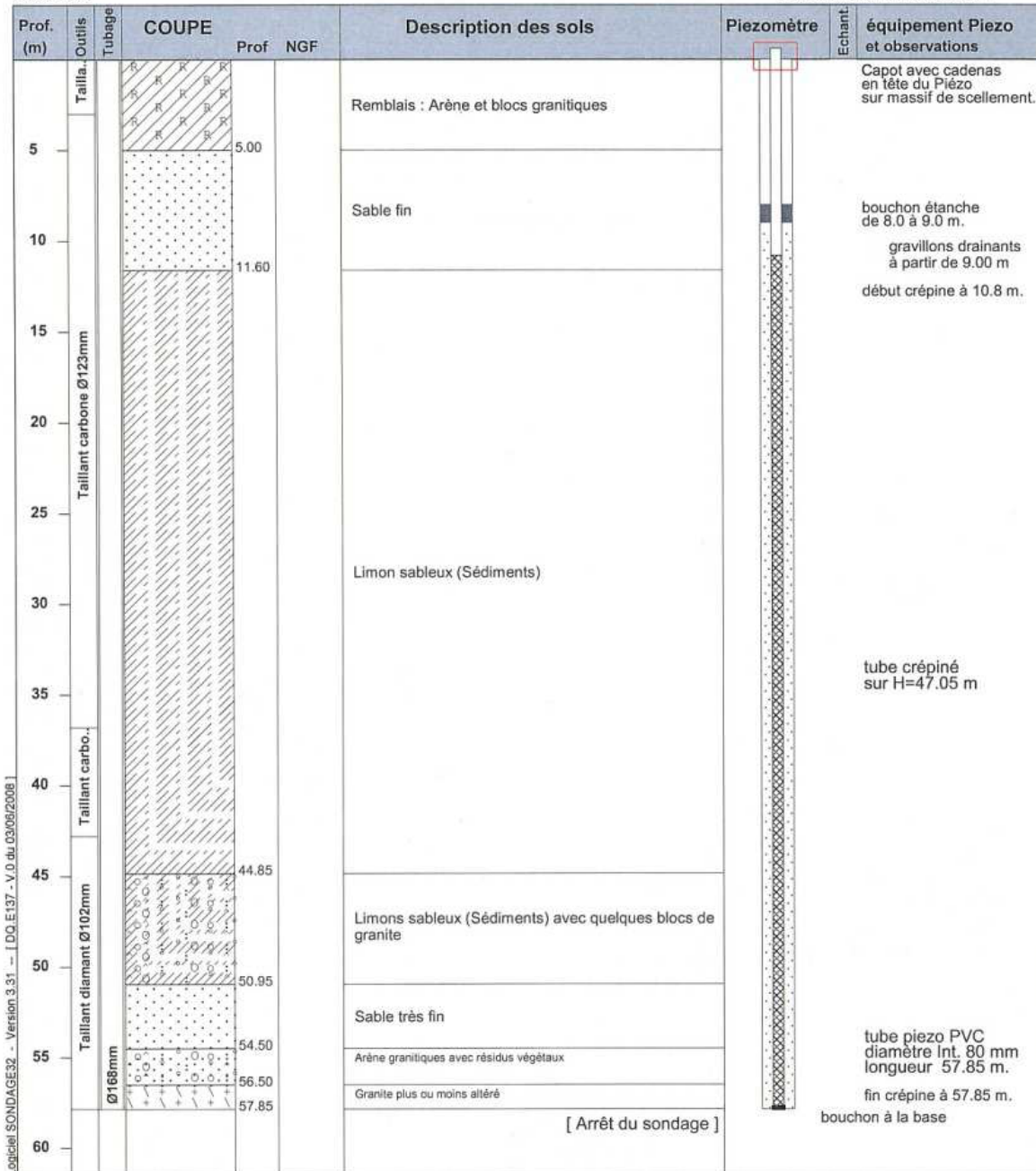
Dossier : SLG2.B.133-2

annexe:



Ech.Prof. /

date travaux: 16-30/04/2011



Sondeuse: Reska 1

Observations : /

Nappe : /
à la date du sondage

Edité le 05/05/2011

Figure 17: Depth profile in the drill hole PZ98 [16]

GINGER
CEBTP

SONDAGE DESTRUCTIF LVG3

Chantier : Sondages carottés et essais de perméabilité

Client : AREVA NC
Dossier : SLG2.B.133

annexe:

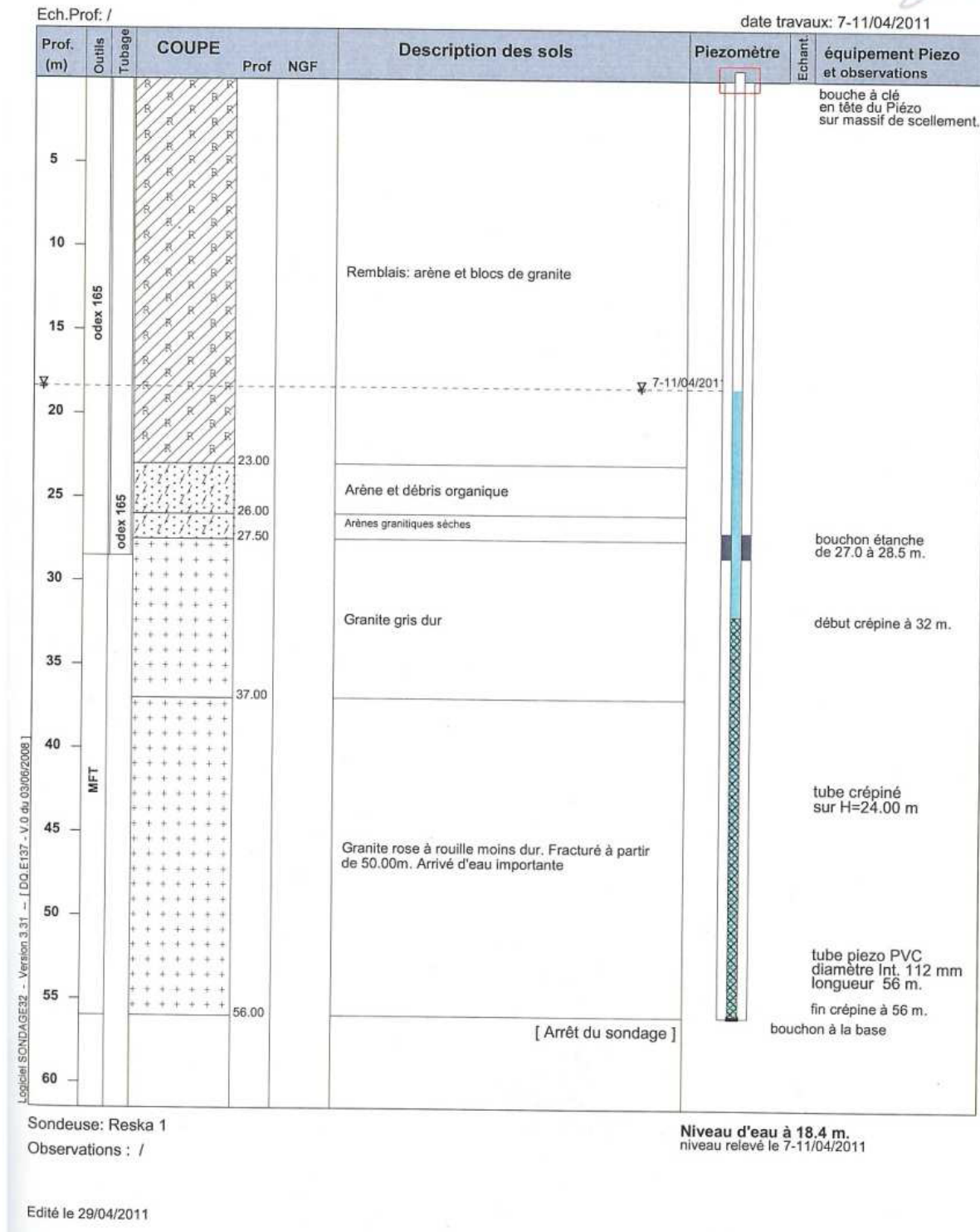


Figure 18: Depth profile in the drill hole PZ95 [16]

GINGER
CEBTP

SONDAGE CAROTTE LVG4

Chantier : Sondages carottés

Client : AREVA NC
Dossier : SLG2.B.133-2

annexe:

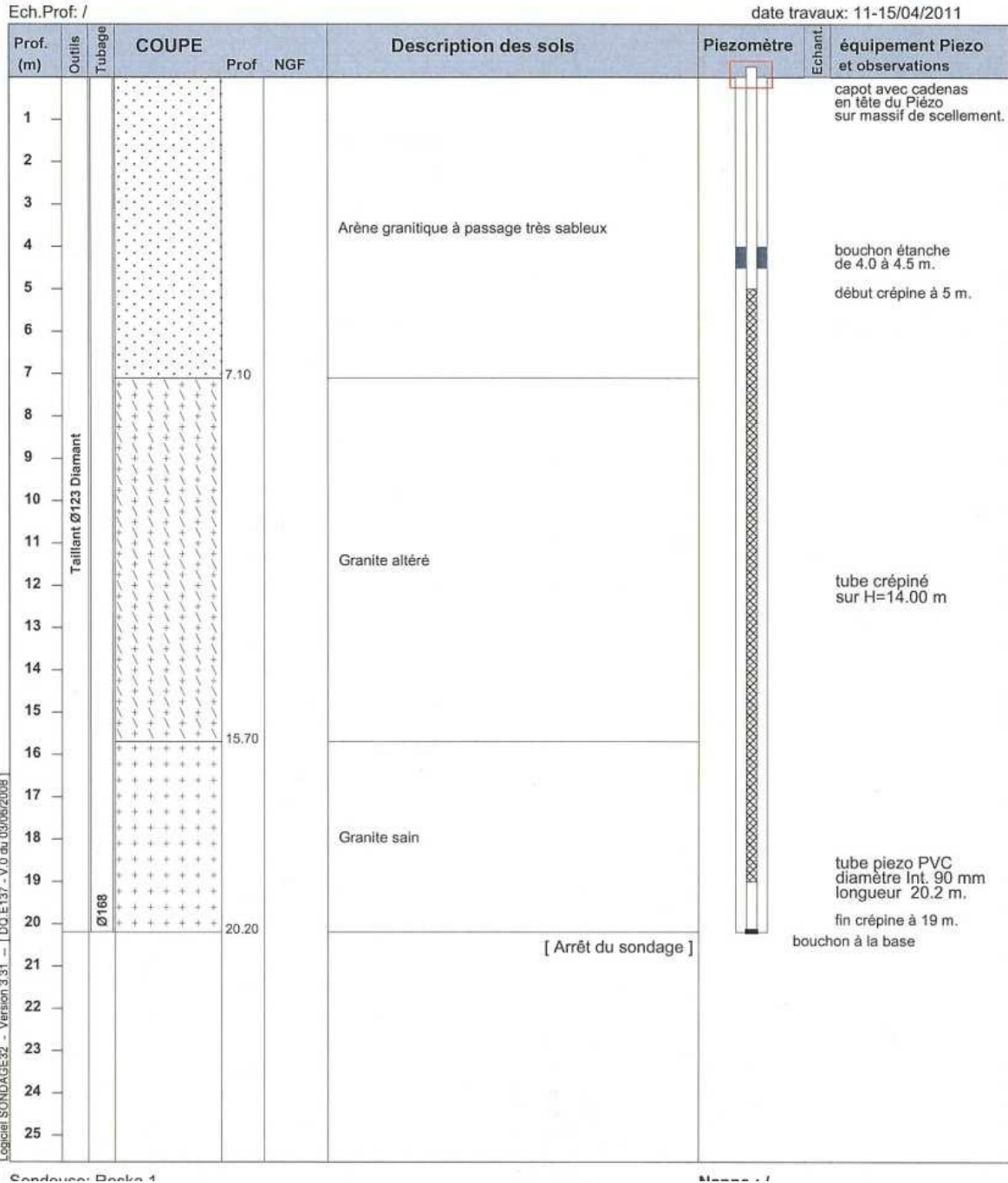


Figure 19: Depth profile in the drill hole PZ96/PZ96B [16]

GINGER
CEBTP

SONDAGE CAROTTE LVG5

Chantier : Sondages carottés

Client : AREVA NC
Dossier : SLG2.B.133-2

annexe:

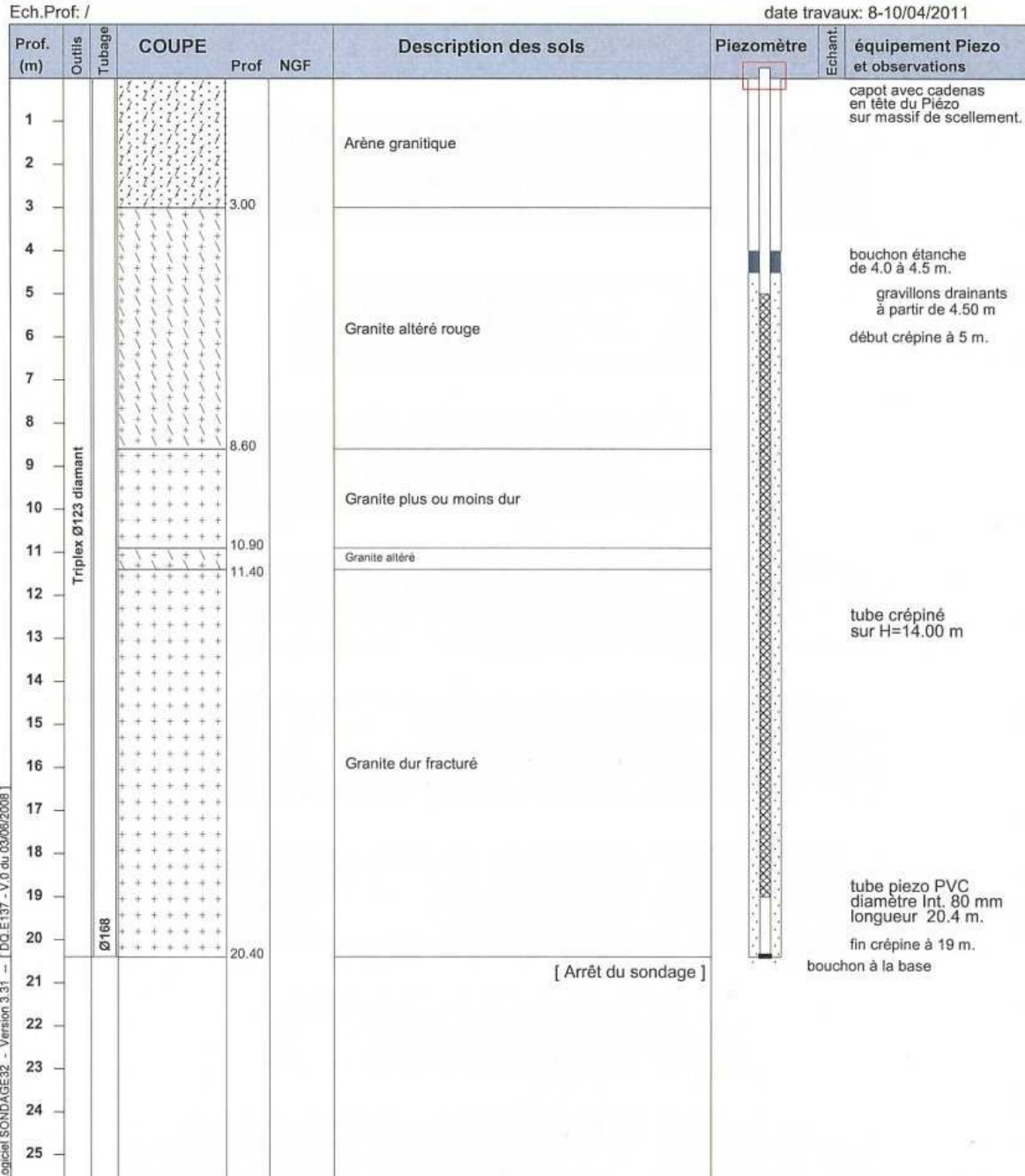


Figure 20: Depth profile in the drill hole PZ94 [16]

Table 8 shows the collected data of the different piezometers with the pump and the gauge. PZ98 and PZ95 are situated lower than the other measuring points, and only PZ98 is located at the top of the residue storage hill Lavaugrasse.

Table 8: Data of the pumping

Piezometer	Depth of the well	Initial groundwater level	Pump rate	Total pumped volume
-	m	m	L/min	L
PZ94	20.9	2.9	7.0	240.0
PZ95	56.8	19.9	8.1 (down to 7.0)	396.0
PZ96	20.8	0.6	4.7 (down to 2.0)	122.0
PZ96B	20.8	0.6	2.0	192.0
PZ98	56.0	39.2	4.7	> 250.0

3.1.1.1 Sampling of Surface Water

Direct removal of the specimen with a sampling vessel.

3.1.1.2 Preparation of the Samplings

These preparations were made for each groundwater and surface water sampling for the later analysis at the hydro-chemical laboratory of the Centre de Géoscience de Mines ParisTech in Fontainebleau. First, the samples were filtered with a Buchner funnel. The filter paper has a pore diameter of 0.45 μm . Then two bottles (50 cm^3) were filled to the brim without bubbles: One with nitric acid (1.5 ml in 150 ml) and one without any extras. The bottles are conserved in a refrigerator box and later in a fridge. The acid field sample is needed for the Atom Absorption Spectroscopy (AAS) and the one without extras for the Ion Chromatography (IC).

3.1.1.3 On-site Analysis

These analyses were done with the same samples which were used for the sampling preparation for the laboratory analyses. Temperature, pH-value, electrical conductivity, dissolved oxygen concentration and redox potential are measured directly with sensors.

The alkalinity is detected by a manual titration with sulfuric acid (0.8 M) in the presence of an indicator (Bromcresol Green-Methyl Red Indicator).

3.2 Laboratory Analyses

Chemical analyses were carried out in the hydro-chemical laboratory of the Centre de Géoscience de Mines ParisTech in Fontainebleau. Radioactive compounds were analyzed by the laboratory of AREVA (Service d'Etudes de Procédés et Analyses, SEPA) next to the closed mining site in Bessines-sur-Gartempe.

3.2.1 Chemical Laboratory of the Centre de Géoscience de Mines ParisTech

The metals (Fe, Zn, Mn, Ni and Al) were analyzed by AAS (Atom Absorption Spectroscopy) and the other anions, cations as well as silicium with an IC (Ion Chromatography).

3.2.1.1 Atom Absorption Spectroscopy

Figure 21 shows the AAnalyst 300 from Perkin Elmer in the laboratory in Fontainebleau. It works with the graphite furnace HGA800 and air-acetylene.

Used standards (contain 2 g/l $Mg(NO_3)_2$ and 2 g/l Palladium as matrix-modifiers) were applied for all elements except Aluminum where only 1 g/l $Mg(NO_3)_2$ was used.

The following Table 9 shows the used monoelement standard for the Atom Absorption Spectroscopy in the laboratory of the Centre de Géoscience in Fontainebleau.

Table 9: Monoelement Standard [18]

Flame	mg/l				
Zn	0.1	0.2	0.5	1.0	2.0
Mn	0.5	1.0	3.0	6.0	-
Fe	1.0	3.0	6.0	10.0	-
Oven	µg/l				
Al	0.0	10.0	20.0	30.0	40.0
Co	0.0	10.0	20.0	30.0	40.0
Pb	0.0	10.0	20.0	30.0	40.0
Fe	0.0	10.0	20.0	30.0	40.0
Cu	0.0	5.0	10.0	15.0	20.0
Ni	0.0	10.0	20.0	30.0	50.0
Cd	0.0	1.0	2.0	3.0	4.0



Figure 21: AAnalyst 300 Perkin Elmer

3.2.1.2 Liquid Ion Chromatography

Figure 22 shows the liquid ion chromatograph DIONEX DX 500 with the gradient pump GP40 and the electrochemical detector ED40. Furthermore are an automated sampler AS40, an absorbance detector AD20 and a chromatography enclosure LC20 are also part of the equipment. The software to control the chromatograph is PEAKNET.

With ion chromatography the anions F^- , Cl^- , NO_2^- , Br^- , NO_3^- , SO_4^{2-} ; and the cations Li^+ , Na^+ , NH_4^+ , K^+ , Mg^{2+} , Ca^{2+} as well as silica SiO_2 were measured.

Table 10 describes the specific measurement conditions in the laboratory of the Centre de Géoscience in Fontainebleau and Table 11 shows the used standards.



Figure 22: LC DIONEX DX 500 with the gradient pump GP40 and the electrochemical detector ED40

SiO₂ (aq) wasn't detected by the electrochemical detector ED40 but with the photometric detector AD20. This method "is based on the absorption of monochromatic light. Detection is made by indirect absorption of a chromophore and post-column reactions." A specific reactant which forms a photosensitive complex with the eluting substances is added at the end of the column. The reactant is forced by the help of an inert gas

Table 10: Measurement conditions liquid ion chromatography [19]

		Anions	Cations	Silica
Flow rate	ml/min	1.2	1.0	1.5
For 1L eluant	g	0.37066 Na ₂ CO ₃	1.33 CH ₃ SO ₃ H	0.92745 H ₃ BO ₃
		0.034 NaHCO ₃	-	576 µl NaOH
For 1L reagent post-column	g	-	-	4.83 Na ₂ MoO ₄
		-	-	12 ml HNO ₃
		-	-	1.73 C ₁₂ H ₂₅ NaO ₄ S
Flow rate post-column	ml/min	-	-	0.5
Pump pressor	psi	1300-1400	1300-1400	1023
Chemical suppressor		ASRS-I 4 mm, works under 100 mA	ASRS-I 4 mm, works under 50 mA	-
Lamp	nm	210, UV low	210, UV low	410, Tungsten low
Electrochemical detector		ED 40, range 10 µS	ED 40, range 10 µS	AD20
Standard basis line		between 15 and 20 µS	between 0.5 and 5 µS	-
Time of acquisition	min	12	10	5.5

Table 11: Different standards for the IC [18]

Cations	mg/l					
	Li+	Na+	NH ₄ ⁺	K+	Mg ⁺⁺	Ca ⁺⁺
1	0.3	35.0	3.0	10.0	10.0	0.5
2	0.05	15.0	0.5	0.5	0.5	2.0
3	0.1	0.5	1.0	1.0	1.0	10.0
4	0.15	1.0	0.1	0.1	0.1	20.0
5	0.2	5.0	2.0	2.0	2.0	40.0
Anions	F ⁻	Cl ⁻	NO ₂ ⁻	Br ⁻	NO ₃ ⁻	SO ₄ ⁻⁻
1	30.0	30.0	1.0	0.6	10.0	5.0
2	1.0	15.0	0.3	0.2	0.5	1.0
3	4.0	7.0	0.1	4.0	0.2	10.0
4	8.0	0.3	2.0	1.0	1.0	30.0
5	10.0	1.0	0.5	2.0	5.0	50.0
Silica						
1	1.0					
2	5.0					
3	15.0					
4	25.0					
5	40.0					

3.2.2 Chemical Laboratory of AREVA (Service d'Etudes de Procédés et Analyses)

At this laboratory at the industrial site Bessines-sur-Gartempe Ra-226 and U-238 were analyzed. The analysis of radium was realized with radon emanometry based on the norm NF M 60-803-1 (Nuclear Energy - Measurement of Radioactivity in the Environment - Water - Part 1: Measurement of Radium 226 Activity in Water by Emanometry) and the analysis of uranium was done by ICP-AES (Inductively coupled plasma – Atomic emission spectrometry) based on the norm NF M 60-805-2 or ICP-MS (Inductively coupled plasma - mass spectroscopy) based on the norm NF M 60-805-4. [20]

3.2.2.1 Radon Emanometry [20]

This analyzing method doesn't analyze radium directly but its decay products. The sample is concentrated by evaporation to 50 ml, and then placed in a fermentation lock. Bubbles of nitrogen are used to chase every present radon nuclide in the sample. This moment is noted as $t = 0$.

The sample is conserved in the fermentation lock for 5 days, to achieve a partial neoformation of radon. New bubbles of the sample are done with the help of nitrogen. The mixture of radon and nitrogen were collected in a scintillator balloon. This instant is noted as $t = 1$.

The next step is the last step before collecting the radon. This step represents waiting until radon 222 is in equilibrium with its direct decay products. The waiting time takes as a minimum three hours. This moment is noted as $t = 2$.

The coating of the scintillating vials is zinc sulfide. When the α -rays of radon 222, of polonium 218 and of polonium 214 bounce at this coating, a light photon is emitted. This shining is detected by the photomultiplier. The activity of the samples is proportional to the number of counted photons. The time of accumulation and the balancing of the decay products in the vial are also included to the calculation of the activity.

3.2.2.2 Inductively Coupled Plasma [20]

A curve of calibration is realized, and then the specimens are diluted until they are within the calibration chart.

Inductively Coupled Plasma - Atomic Emission Spectrometry

“After purification the sample, it is nebulised. The aerosol product is transferred in plasma which, using atomic excitation emits spectrum lines that are characteristic of the element being researched. Emission intensity is proportional to concentration. [21]”

Inductively Coupled Plasma - Mass Spectroscopy

“Measurement using inductive-coupled plasma mass spectrometry (ICP-MS) quantifies the number of atoms of each isotope of elements present in the sample. Conversion in radioactivity is then possible using the value for specific activity (Bq/g) for each radioactive isotope. Uranium 233 is used as a tracer because no mass interference is observed with isotopes 234, 235, 236 and 238. [21]”

3.3 Simulation

3.3.1 Description of the Simulation Program HYTEC

A simulation was generated by the program HYTEC, which was developed by scientists of Mines ParisTech in 1993. HYTEC is a modular platform simulation and mainly composed of a hydrodynamic module (R2D2), a reaction module (CHESS) and a coupler. The approach is easily scalable and coupling with other modules is being considered.

This program is “currently used for groundwater pollution studies, safety assessment of nuclear waste disposals, geochemical studies and interpretation of laboratory column experiments. It is a coupled reactive transport code and evaluates groundwater flow paths, and simulates the migration of mobile matter (ions, organics, colloids) subject to geochemical reactions. The code forms part of a module-oriented structure which facilitates maintenance and improves coding flexibility. In particular, using the geochemical module CHESS as a common denominator for several reactive transport models significantly facilitates the development of new geochemical features which become automatically available to all models. The common denominator is the geochemical module CHESS, written in object-oriented C++ and highly optimized for coupling purposes. All function calls require specific classes; hence calling the library also requires a C++ code. Therefore, all non-C++ codes linked to CHESS communicate through specific interface modules. JCHESS is an exception: written in java, JCHESS provides a graphical user interface to run CHESS as a stand-alone geochemical code. [22]” The global structure of HYTEC is presented in Figure 23. For the simulation only HYTEC, the hydrodynamic module R2D2, the reaction module CHESS and a coupler, were used.

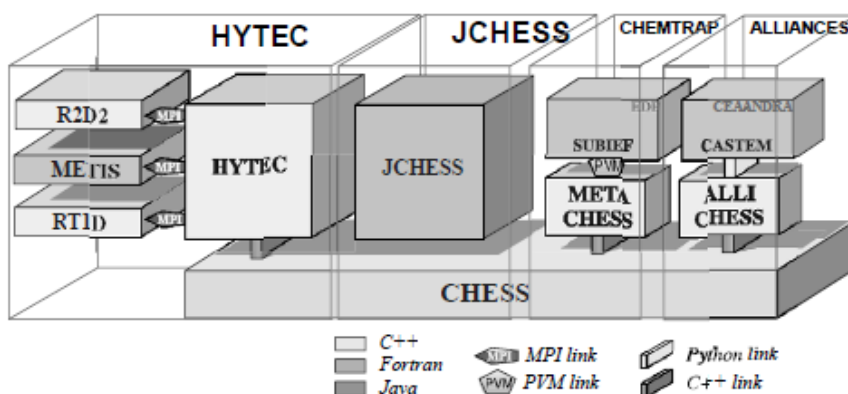


Figure 23: Global structure of HYTEC and related simulation tools based on CHESS [22]

3.3.2 Collecting of Data for the Simulation

For successful simulation large amounts of data are needed. Unfortunately there wasn't enough time to include all necessary information. That's why I only considered using the following data:

The simulation area, shown in Figure 24, is a cross section of a part of the industrial site Bessines.



Figure 24: Simulation profile

The model includes several hydrological units. The creation of the model and the feed will be described beneath the Figure 25.

- The storage of residues of Lavaugrasse (red) and its dike (blue)
- The waste piles from Vieux Moulin to the river Gartempe (green)
- The granitic sand under the waste piles and Lavaugrasse storage (brown)
- The fractured granite under the granitic sand (light blue),
- And as foundation the unaltered granite (pink).

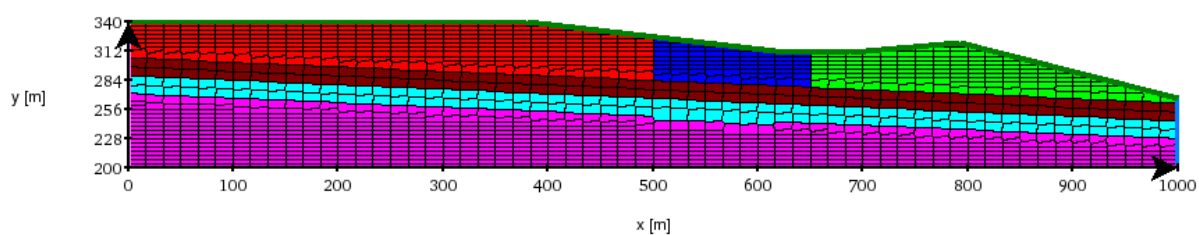


Figure 25: Details of the model section. (red: Lavaugrasse, residues; blue: Dike, residues; green: Vieux Moulin, waste piles; brown: weathered granite; light blue: fractured granite; pink: unaltered granite)

The orientation as shown in the Figure 24 of the model (Figure 25) is from north-north-east to south-south-west. The geometry is based on ancient maps of this area before mining activities started and after closing down of the mining site. To simplify the simulation data were rounded up or rounded down to a full integer. Unfortunately the available notes were not completed, so there are no serious data about the precise construction of the existing granite layers. Therefore, some suggestions were done. The basic geological parameters like porosity and permeability were taken from another report on the industrial site of Bessines-de-Gartempe and are shown in Table 12. [16]

The geological underground was treated as a homogenous area with hydrodynamic dispersion of 1 m (pore aquifer) and a diffusion coefficient of $1 \cdot 10^{-10} \text{ m}^2/\text{s}$. The hydrodynamic dispersion is at the macroscopic level “the spreading of the solute front during transport resulting from both mechanical dispersion and molecular diffusion or the dynamic dispersion of fluid particles in flow through a porous medium due to velocity changes in the pore channels. [23]” As basic geological data for the simulation are those taken from Table 12.

Table 12: Basic geological parameters for the simulation [16]

	Porosity	Permeability	hydrodynamic dispersion	diffusion coefficient
	-	m^2	m	m^2/s
Lavaugrasse	0,35	$6 \cdot 10^{-7}$	1	10^{10}
Vieux Moulin	0,35	$1 \cdot 10^{-6}$	1	10^{10}
Dike	0,05	$5 \cdot 10^{-7}$	1	10^{10}
Wheated granite	0,05	$1 \cdot 10^{-6}$	1	10^{10}
Fractured granite	0,05	$1 \cdot 10^{-6}$	1	10^{10}
Unaltered granite	0,05	$5 \cdot 10^{-7}$	1	10^{10}

The chemistry of Lavaugrasse (residues) was taken from a report about the mining site of Bellezane [24] in combination with the results of the chemical analysis of the piezometer PZ98. Bellezane is a mining site close to the industrial site of Bessines with a similar geological composition. These parameters were used because of the lack of time to create a

specific model. For the chemistry of Vieux Moulin and the data of the analysis of the PZ95 were taken.

These parameters were the feed for the geochemical module CHESS to find the equilibrium between the water and minerals of the different geochemical zones. The minerals in equilibrium are shown in Table 13.

Table 13: Minerals in equilibrium

Lavaugrassse	Vieux Moulin, Dike	Weathered, Fractured, Unaltered Granite
minerals in equilibrium		
Quartz, Kaolinite, Gypsum, Dolomite, Fluorite, Siderite, Rhodochrosite, Uraninite and Soddyite	Quartz, Kaolinite, Gypsum, Dolomite, Fluorite, Siderite, Rhodochrosite, Uraninite and Soddyite, Muscovite and Fluorite	Quartz, Muscovite, Argile, Feldspar, Pyrite, Sulfates

The used composition of the rain was an average data of the rain at the Massif Central and is shown in Table 14. The parameters are rounded and the values for Magnesium, Potassium and SiO₂ (aq) are negligible. The simulated amount of precipitation was 1050 mm/year.

Table 14: Composition of the rain at the Massif Central [25]

pH	6,37	-
Cl ⁻	1	g/l
Na ⁺	1	g/l
Ca ²⁺	1	g/l
HCO ₃ ⁻	2	g/l
O ₂ aq	11	g/l

The duration of the simulation was 10 years to simulate the evolution of the water drainage and distribution from the end of remediation to date. Actual data were used to for the boundary conditions (the highest piezometer PZ98) and to verify if the scenario matches with the actual observations. [26]

4. Chemical Composition of Surface and Ground Water

In this chapter the different results of the in Chapter Fehler! Verweisquelle konnte nicht gefunden werden. presented analysis (on-site analysis, the analysis of the laboratories) as well as the results of the simulation.

4.1 Results of the On-Site Analyses

As shown in Table 15 are the temperatures very similar to each other with an average temperature of $12.37\text{ }^{\circ}\text{C} \pm 1.85\text{ }^{\circ}\text{C}$. The pH value is throughout acidic, from the weakly acidic PZ98 (pH = 6.3) at the storage of residues of Lavaugrassse to the highly acidic SIBGAL (pH = 3.8) which are waters from the effluent of the drainage of the underground mining site Vieux Moulin. There, mining activity exposed the rocks to the atmosphere. So fresh oxygen entered the mine and Pyrite (FeS_2) oxidized according to the following formula:



Table 15: Results of the on-site analysis in Bessines (T... Temperature, EC... Electrical Conductivity, DO ... Dissolved Oxygen, Eh...Redox Potential)

	T	pH	EC	DO	Eh	Alkalinity
	$^{\circ}\text{C}$	-	μS	ppm	mV	mg/l
PZ 94	11.5	4.8	1,596	1.9	20.8	3.0
PZ95	13.6	5.2	2,770	0.1	28.2	64.0
PZ 96	12.5	4.9	2,107	1.5	66.9	13.0
PZ96 B	12.6	4.9	2,107	0.9	73.8	-
PZ98	13.0	6.3	3,830	0.4	22.4	374.0
SIBGAL	12.2	3.8	1,641	2.9	8.4	0.0
SIBDOB	12.1	5.3	1,958	3.6	15.3	14.0
SIBDOB 2	11.5	5.3	644	3.6	24.9	7.0

The electrical conductivity values are in general not very high. Like for the pH value the sample PZ98 has also the highest. The concentration of dissolved oxygen is very low. It seems that they are too low because of water pumping during the sampling.

The redox potential depends on dissolved oxygen and pH value, when the pH value decreases, the redox potential increases. The redox potential has a vast range between 8.4 mV up to 73.8 mV.

In general, the higher the redox potential, the more oxidative is the system. The dissolved oxygen concentration has an influence on the solubility of chemical compounds.

Alkalinity is the buffering capacity of a water body. It measures the ability of water bodies to neutralize acids and bases thereby maintaining a fairly stable pH. If an area's geology

contains large quantities of calcium carbonate (CaCO_3 , limestone), water bodies tend to have a higher alkalinity.

The samples of PZ94, PZ95 and PZ96/PZ96B are at the area of the dikes and PZ98, SIBGAL, SIBDOB, SIBDOB2 are samples from treatment residue storages. The composition of the soils is different.

The piezometer PZ98, situated at the middle of the treatment residue storage Lavaugrass, has the highest alkalinity as well as the highest electrical conductivity and the most alkaline pH value but a moderate redox potential. The soil is very sandy and contains a lot of clay. This is a fine grain material with a poor water capacity and a moderate pollutant accumulation. That means a progressively increasing of concentrations of pollutions in the soil.

The soil is very granitic of the piezometers PZ95, PZ96/PZ96B and PZ94. They contain different types of granite and its alteration states. At all three piezometers, PZ94 shows the lowest alkalinity and PZ95 the highest.

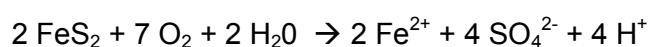
The samples of the surface water origin of the underground gallery of the underground mine Vieux Moulin (SIBGAL) and of the treatment residue storages of Brugeaud (SIBDOB and SIBDOB2). The alkalinity is at all three not very high but the very lowest alkalinity has the water of SIBGAL (0.0 mg/l). It has also the lowest pH value (3.8).

4.1.1 Results of the Laboratory of the Centre de Géoscience from Mines ParisTech

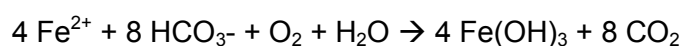
The results of the analysis are shown in Table 16. The anions NO_2^- and Br^- are continuously under the limit of quantification. The cations NH_4^+ and Li^+ occur only in minimal amounts. The values of nitrate ion are higher than the NH_4^+ values which indicate a nitrification process. The nitrite ion values are under the limit of quantification.

The alkaline earth metals leach out at the present of bicarbonate and high pH value. In the last preceding paragraph it was announced that PZ98 has the highest pH value, a result of these high pH value is a high bicarbonate value.

The results clearly show the mineral composition of the examined area. The following elements are part of several minerals which are the composition of the granite in the area of Bessines. Quartz (SiO_2) is a component of granite and aqueous silica is analyzed in every water sample. Aluminium is part of feldspar and muscovite (a kind of mica). Because of weathered pyrite (FeS_2) a higher SO_4^{2-} and a higher iron concentration can be observed.



Fe(II) is readily soluble in an acidic environment with less oxygen and less organic. When Fe(II) oxidizes to Fe(III) it precipitate as iron hydroxide bounded with further heavy metals (Mn, Ni, Zn):



Biotite as well as pyrite has iron in reduced form which will be oxidized in an O_2 weathering milieu. There the labile bonding of the mineral will be destroyed and Fe(II) released. Mn and Al compounds have very similar weathering processes.

In strong acidic milieus ($\text{pH} < 4$) aluminum is still in solution. The sample of SIBGAL is very acidic ($\text{pH} = 3.8$) and has the highest value of aluminum. It is in the range of the aluminum buffer area through dissolution of Al-OH and release of Al^{3+} . In weak acidic milieu SiO_2 and aluminum hydroxides precipitate as kaolinite.

The reaction time of the water with silicate rock is very slow, so that low values of silica ($< 7 \text{ mg/l}$) indicate a long contact time between the water and the rocks. [27] The values are apart from PZ94 and SIBDOB2 always higher than 7 mg/l and they are also very close to this limit. The highest silicate value is from SIBGAL the water from the underground mine Vieux Moulin.

Table 16: Results of the analysis of the laboratory of the Centre de Géoscience in Fontainebleau

mg/l	2012	PZ94	PZ95	PZ96	PZ96-B	PZ98	SIBDOB	SIBDOB2	SIBGAL
Anions	HCO_3^-	3.66	78.08	15.86	-	456.28	17.08	8.54	0.00
	F^-	1.34	< 0.20	< 0.20	< 0.20	< 0.20	6.39	2.22	4.29
	Cl^-	28.61	117.89	22.75	23.27	113.34	30.25	7.98	17.85
	NO_2^-	< 0.20	< 0.20	< 0.20	< 0.20	< 0.20	< 0.20	< 0.20	< 0.20
	Br^-	< 0.20	< 0.20	< 0.20	< 0.20	< 0.20	< 0.20	< 0.20	< 0.20
	NO_3^-	5.29	< 0.20	9.43	9.13	< 0.20	4.66	2.52	6.89
	SO_4^{--}	662.62	1271.14	998.03	1067.54	2029.61	881.19	255.27	744.22
Cations	Li^+	0.02	0.20	< 0.20	< 0.20	0.32	0.14	< 0.20	0.12
	Na^+	51.13	173.54	77.04	78.51	137.02	51.48	13.42	37.98
	NH_4^+	< 0.2	< 0.20	< 0.20	< 0.20	8.33	1.73	< 0.20	< 0.20
	K^+	8.49	9.09	13.04	13.49	28.24	11.72	4.99	9.40
	Mg^{++}	59.89	116.02	69.45	72.52	163.13	59.54	12.28	54.43
	Ca^{++}	209.50	371.61	330.49	340.40	588.67	331.38	91.77	239.05
	Fe	0.03	6.029	0.05	0.09	300.25	6.40	0.03	0.22
	Zn	0.09	0.34	0.14	0.17	0.09	0.15	0.06	0.39
	Mn	7.59	13.95	0.49	0.54	23.94	8.79	1.98	7.85
	Ni	0.01	0.02	0.02	0.02	0.01	0.02	0.01	0.02
	Al	2.58	1.56	0.47	0.63	0.69	3.15	1.97	14.44
Silica	$\text{SiO}_2 \text{ (aq)}$	6,53	12,56	12,46	12,64	15,31	13,38	6,76	17,17

In 2010 another study on the hydrogeochemical situation of the three sites Brugeaud, Lavaugrassse and Montmassacrot was done [13]. Three samples were taken of the same sampling field. Table 17 shows the samples of SIMOGAL, SIBDOB and SIBDOB2 of 2010 and 2012.

Table 17: Comparison of samples

		2010			2012		
		SIBDOB [13]	SIBDOB2 [13]	SIBGAL [13]	SIBDOB	SIBDOB2	SIBGAL
pH	-	5.70	6.58	4.12	5.3	5.3	3.8
HCO ₃ ⁻	mg/l	30.00	118.00	0.00	17.08	8.54	0.00
F ⁻	mg/l	5.79	5.63	4.78	6.39	2.22	4.29
Cl ⁻	mg/l	42.01	58.81	19.54	30.25	7.98	17.85
NO ₃ ⁻	mg/l	4.77	3.33	10.57	4.66	2.52	6.89
SO ₄ ²⁻	mg/l	1138.82	1359.96	870.61	881.19	255.27	744.22
SiO ₂	mg/l	15.21	10.37	10.99	13.38	6.76	17.17
Na ⁺	mg/l	57.08	71.75	34.78	51.48	13.42	37.98
NH ₄ ⁺	mg/l	<0.1	4.50	<0.1	1.73	< 0.20	< 0.20
K ⁺	mg/l	12.34	14.44	8.78	11.72	4.99	9.40
Mg ²⁺	mg/l	52.84	68.49	45.67	59.54	12.28	54.43
Ca ²⁺	mg/l	393.79	484.40	256.98	331.38	91.77	239.05
Al	mg/l	16.92	3.40	13.22	3.15	1.97	14.44
Fe	mg/l	0.05	0.02	0.0006	6.4	0.03	0.22
Mn	mg/l	12.50	19.56	10.54	8.79	1.98	7.85
Ni	mg/l	0.02	0.02	0.04	0.02	0.01	0.02
Zn	mg/l	0.13	0.035	0.49	0.15	0.06	0.39
Usol	mg/l	0.48	0.05	1.56	0.29	0.13	1.07
Uinsol	mg/l	0.17	0.12	<0.001	0.133	0.044	0.003
Rasol	Bq/l	1.28	1.07	2.74	1.75	0.59	2.29
Rainsol	Bq/l	0.01	0.17	<0.02	0.07	0.18	0.03

The concentrations of SIBGAL didn't change very much. Two things are remarkable, the pH value has lowered from 4.2 to 3.8 and the value of SO₄²⁻ has become considerably less.

The concentrations of SIBDOB were also almost steady. Significant changes are the decreases of SO₄²⁻ as well as of some metals Al, Fe and Mn.

In contrast to the concentrations of SIBDOB2 which have changed a lot. The pH value has also lowered from 6.58 to 5.3. Nearly all concentrations were lower in 2012 than in 2010. Very notable are the values of HCO₃⁻, Cl⁻, SO₄²⁻, Na⁺, K⁺, Mg²⁺, Ca²⁺, Mn and Ra_{sol} because they were twice or more the value of 2012. They don't agree because some work was done between the samplings in the drainage area of SIBDOB2.

4.1.2 Results of the Laboratory of AREVA at the Industrial Site of Bessines

The results of the laboratory of AREVA (Service d'Etudes de Procédés et Analyses, SEPA) next to the closed mining site in Bessines-sur-Gartempe are shown in Table 18. There the content of soluble and insoluble uranium and radium are analyzed.

In the nature, mainly tetravalent and hexavalent uranium ions exist. The tetravalent uranium is only under high acidic and very reducing conditions soluble. The hexavalent uranium is soluble in acidic and alkaline conditions. [28]

The Figure 26 shows an Eh-pH-diagram of uranium which presents the thermodynamic stability areas of different species in an aqueous solution. It shows the existence of solid uranium at low Eh and the dominance of dissolved uranium at higher Eh values. The Eh values of the samples are very low so they are only schematic presented at the figure but they are mostly situated in the uraninite area. As a result, most of the uranium is principal available in solid phase as UO_2 . This form is rather stable in environmental conditions. [29] The presence of kaolinite shifts the balance particularly. It makes the presence of uranyl ion possible although there is a low Eh potential. The same effects should be possible by the presence of other natural water system. It has to be repeated that UO_2 is the stable uranium species at low Eh potential but colloidal solids form could be the mobile phase. [30]

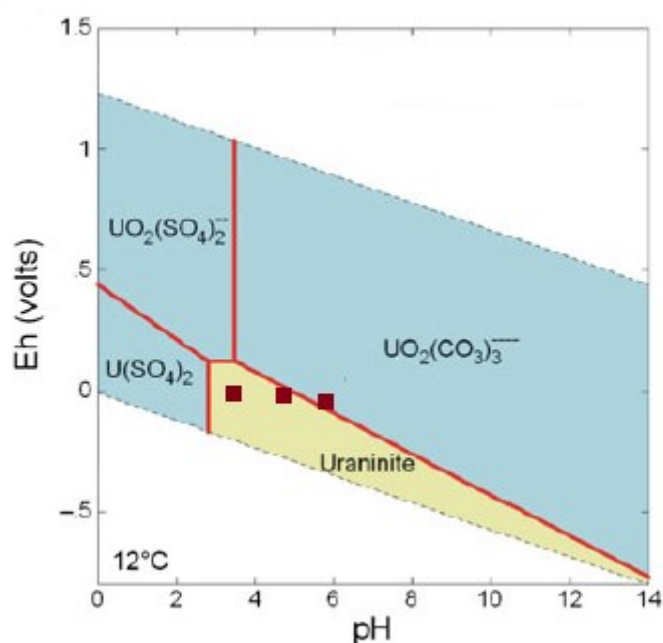


Figure 26: Eh-pH-diagram of uranium and its species $\text{U}^{4+} = 0.01 \text{ mg/l}$, $T = 12^\circ\text{C}$, $P = 1.013 \text{ bars}$, $a[\text{main}] = 10^{-1.88}$, $a[\text{H}_2\text{O}] = 1$, $a[\text{SO}_4] = 10^{1.89}$, $a[\text{HCO}_3] = 10^{2.26}$ [31]

Radium is always bivalent, forms mostly simple salts and is chemical similar to barium. Radiumhydroxide is the most soluble of the alkaline earth hydroxides and radium sulfate is the most insoluble of the alkaline earth sulfates and probably the most insoluble radium compound known. [32]

As a repetition the limits for a direct discharge are 0.37 Bq/l for Ra-226 soluble, 3.7 Bq/l for Ra-226 insoluble and 1.8 mg/l for U-238 soluble [8]. As a result several Ra-226 values are exceeded. The concentration of soluble Ra-226 in the samples PZ98, SIBDOB, SIBDOB2 and SIBGAL and the concentration of insoluble Ra-226 of PZ98 are overranged. PZ98 is the piezometer in the center of Lavaugrasse it is refilled with treatment residues and is situated in a natural depression. The axes of the drainage system are beneath Lavaugrasse which collect most waters. These waters which percolate through the waste tips of Lavaugrasse and Vieux Moulin accentuate downstream to the site at the points SIBDOB and SIBDOB2.

The mining site in Schlema-Alberode is also a vein deposit thus granite related deposit from the type second type. The basic conditions are the same as in Bessines-sur-Gartempe. The concentrations of Ra and U of the waste-tips of Schlema-Alberode are: the concentration of Ra is between 0.3 Bq/g – 5.0 Bq/g and the concentration of U is < 100 mg/kg. When the assumption is made that kg = l are the values of uranium in Schlema-Alberode higher than in Bessines-sur-Gartempe but the concentrations of radium higher than in Bessines-sur-Gartempe.

Table 18: Results of the analysis of the laboratory of AREVA next to the closed mining site in Bessines-sur-Gartempe

			PZ94	PZ95	PZ96	PZ96B	PZ98	SIBDOB	SIBDOB2	SIBGAL
soluble	mg/l	U-238	0.03	0.14	0.03	-	0.02	0.29	0.13	1.07
	Bq/l	Ra-226	0.14	0.36	0.09	-	1.72	1.75	0.59	2.29
insoluble	mg/l	U-238	<0.001	0.004	0.002	-	0.004	0.133	0.044	0.003
	Bq/l	Ra-226	0.02	0.02	0.02	-	4.28	0.07	0.18	0.03

4.2 Piper-Diagram

The concentration of the major ions in the analyses samples are plotted in a piper diagram by a freeware program called GW-chart (http://water.usgs.gov/nrp/gwsoftware/GW_Chart/GW_Chart.html). This is a program of the U.S. geological survey water division to create graphs for groundwater studies.

A piper diagram represents different proportions. It presents relations between anions and cations, standing alone in a triangle as well as combined in a rectangle.

The feed for a piper diagram are several cations and anions: Ca^{2+} , Mg^{2+} , Na^{2+} , K^{+} , CO_3^{2-} , HCO_3^{-} , Cl^{-} , SO_4^{2-} and TDS (total dissolved solids).

EXPLANATION

- PZ94
- PZ95
- PZ96
- PZ96B
- ▲ PZ98
- △ SIBDOB
- × SIBDOB2
- ★ SIBGAL

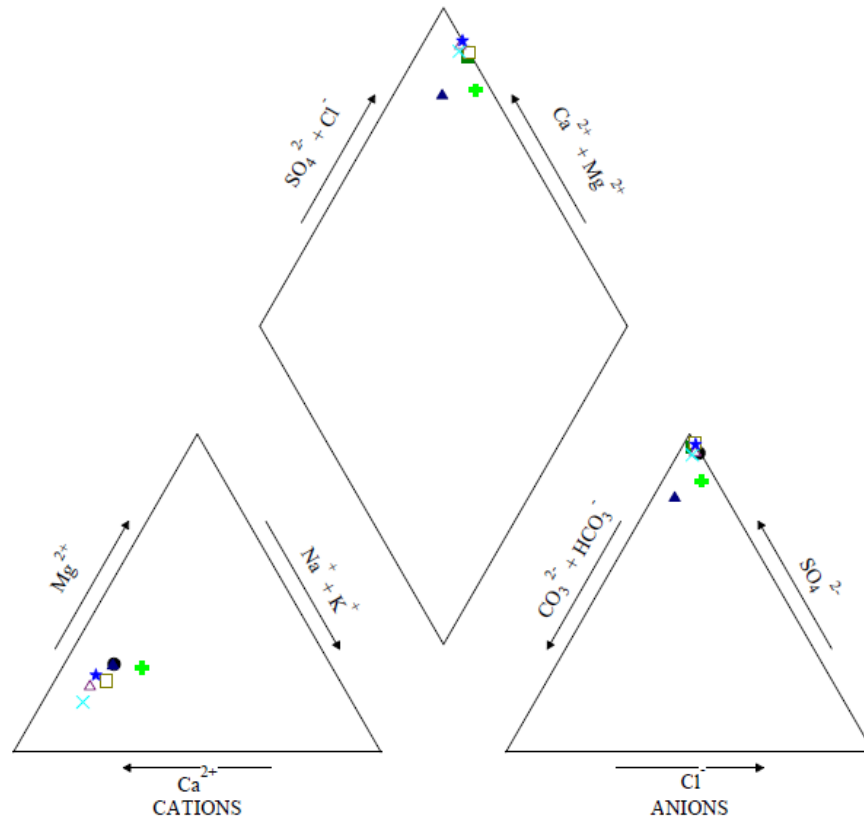


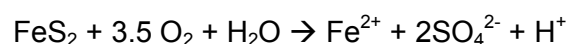
Figure 27: Piper-diagram of the water samples

All of them are very close together at the piper-diagram and the distances as well as the different charging of the ancient mining parts are negligible. The position of the symbols in Figure 27 show a predominant sulfuric water as well as that the aquifer is young and has a high regeneration fraction that means it can be easily affected by diffuse furnish from the surface.

The results of the piper diagram (Figure 27) represent the geology of the area very well. The rectangular shows very well a predominant sulfuric water.

- Anions:

The high ratio of SO_4^{2-} comes, as former described, from the weathering of pyrite which produces acid water:



- Cations:

The hydronium ion forces dissolution of the granite. Granite consists of quartz, feldspar and mica. Mica comprises of biotite and muscovite. Biotite and muscovite are common phyllosilicate minerals with their general chemical formula: $\text{K}(\text{Mg,Fe})_3(\text{AlSi}_3)\text{O}_{10}(\text{OH})_2$ and

$KAl_2(AlSi_3)O_{10}(OH)_2$. Feldspar ($KAlSi_3O_8$; $NaAlSi_3O_8$; $CaAl_2Si_2O_8$) is a very common mineral in the earth crust. Quartz SiO_2 is after feldspar the most common mineral in the world.

This dissolution implies release of Ca^{2+} and Mg^{2+} , and a rise of their concentration in the water. They form with CO_3 atmospheric calcite $CaCO_3$ as well as dolomite $CaMg(CO_3)_2$. As mentioned in chapter 2 there are 1-2% carbonates in the rocks resulting from sulfuric attack and neutralization processes. This diagram shows well the presence of carbonates.

4.3 HYTEC Simulation

The results of the HYTEC simulation confirm the results of the chemical analysis shown in the Piper-diagram above.

The structure is as follow: a figure with three illustration of the evolution of the concentration of dissolved species during the process of the simulation. The duration of the simulation is 10 years after the end of the remediation, this simulates the present time. The simulation shows the evolution of water drainage.

The simulation for the minerals shows a measure for the (contact) boundary layer between the solution and the certain mineral.

4.3.1 Flow Rate

The flow rate in Figure 28 is over the simulation time of 10 years in every direction constant. The direction of the stream is continuous from Lavaugrasse to the river Gartempe. The highest flow rate is in the zone of weathered granite because of the good permeability and porosity of this zone. The feed is the rain and a spring behind the sector Lavaugrasse.

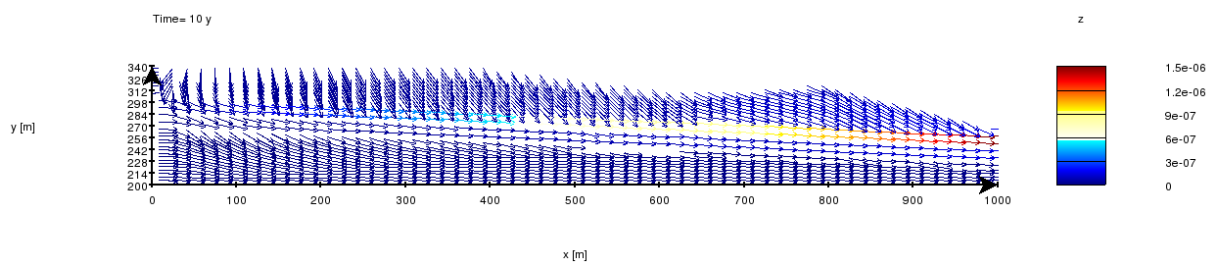


Figure 28: Flow Rate (m/s)

4.3.2 Evolution of the pH value

Figure 29 shows the evolution of the pH value during 10 years. The pH value starts equally among 5.5 to 6.0. Knowing the geological setting of the site and using the rain different ions are washed out of the site. As a result the acidic ions enter the groundwater and acid mine drainage is obtained. The illustration shows that the dike because of his high porosity is the weak point. There the decrease of the pH happens in a short period of time.

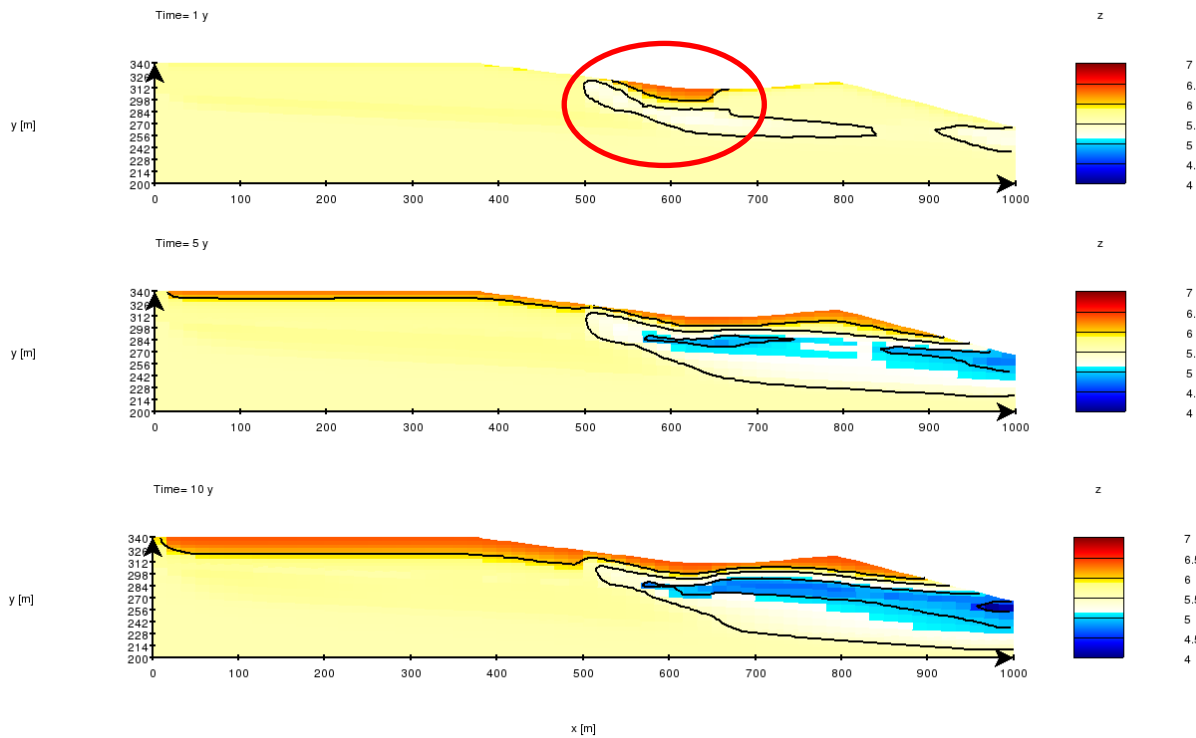


Figure 29: Evolution of the pH value

4.3.3 Sulfate

Figure 30 shows the evolution of the sulfate ion concentration at the industrial site of Bessines-sur-Gartempe. Weathered pyrite is the source of dissolved sulfate ions. The dissolution of pyrite results from the exposure to atmospheric and dissolved oxygen and from the reaction with rain water. It is known that the highest concentration of SO_4^{2-} (Comparison Table 16 PZ98) is at Lavaugrasse which is shown at the first illustration. At the second picture, five years after the start of the simulation, it looks like a spreading leachate plume. The highest concentration of sulfate within the aquifer is below and adjacent to the entering spot. The permeability of the adjacent soil areas is very well so the sulfate can dilute quickly into the subjacent soil formation (weathered and fractured granite zone) to the basin of the river Gartempe. At the third picture, 10 years after the simulation, the diffusion of high concentrated sulfate is widely advanced to the deeper soil layers and to the river border.

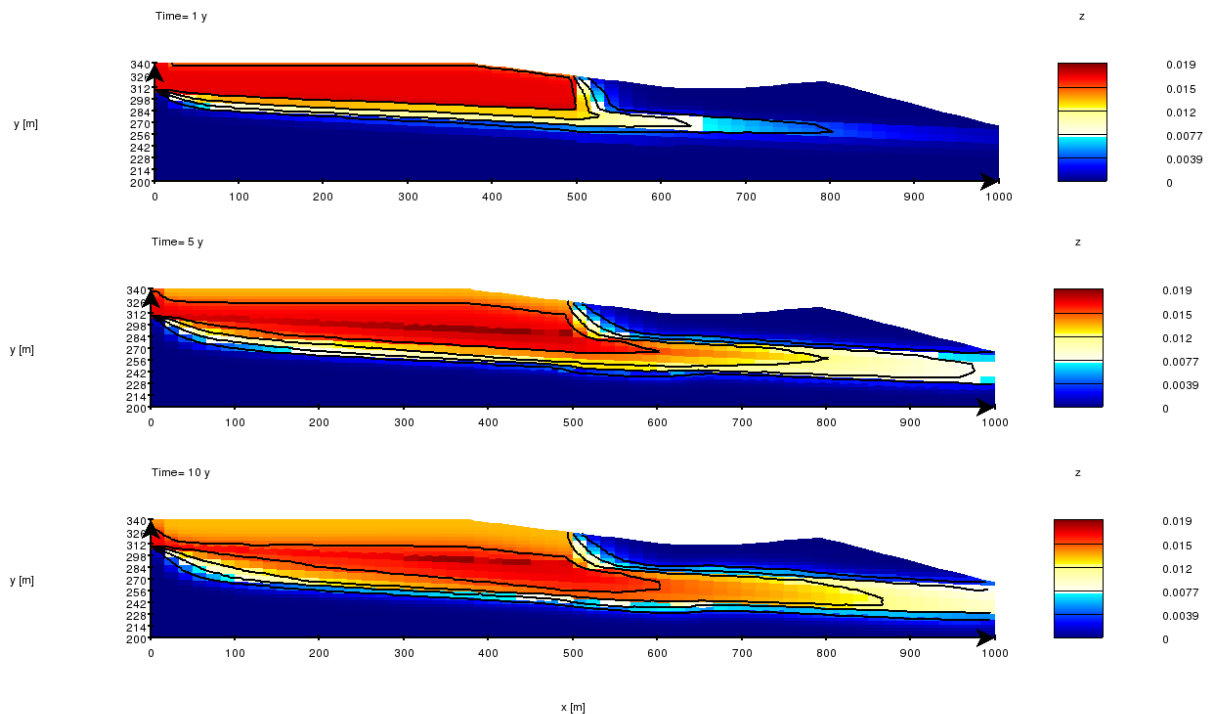


Figure 30: Evolution of the Sulfate Ion (mol/l)

4.3.4 Muscovite dissolution and precipitation

Figure 31 shows the evolution of the mineral muscovite, a type of mica. Muscovite is in equilibrium with the whole area except of the treatment residue storage Lavaugrassé. The weak point with a good permeability is as former described the border to the weathered granite zone. Through the weathering of the major mineral Muscovite $KAl_2[(OH,F)_2AlSi_3O_{10}]$ results from releasing K^+ -ions new minerals. The immobile components aluminum and silica are left over and precipitate as Kaolinite. These processes are shown in the three illustrations.

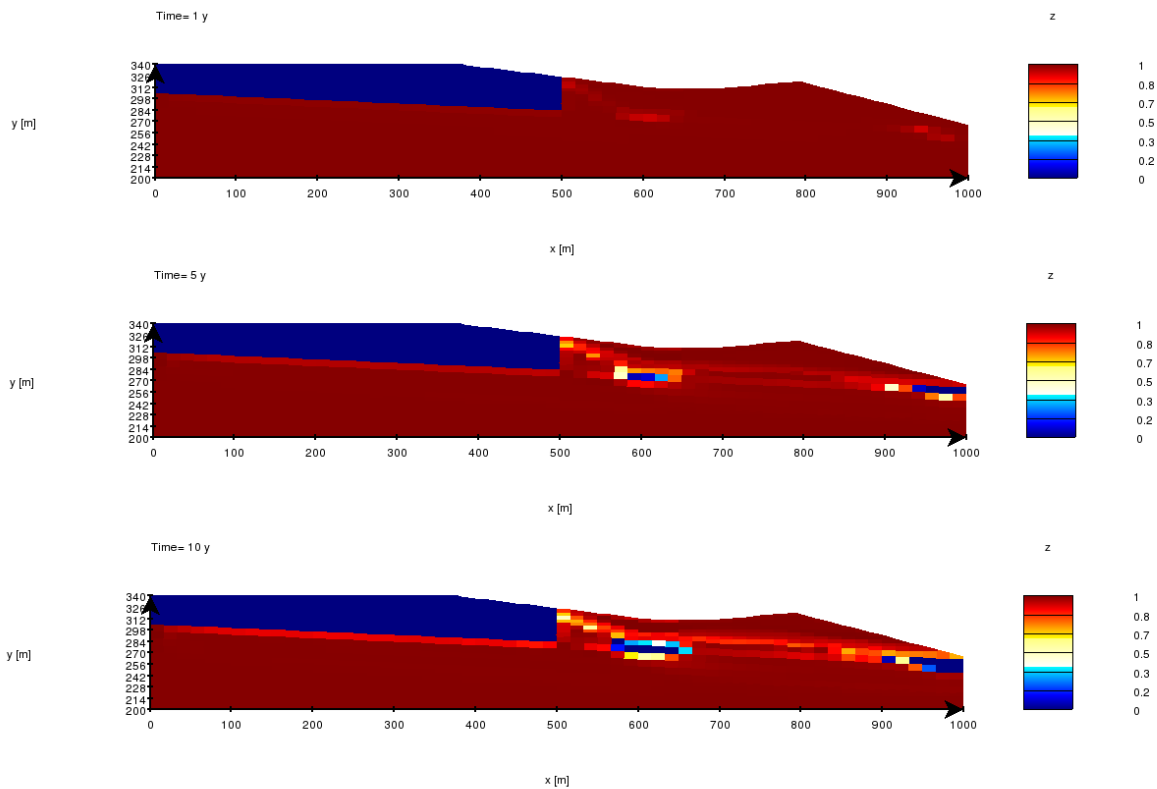
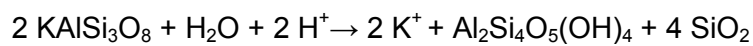
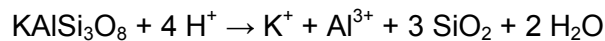


Figure 31: Concentration of Muscovite (mol/l)

4.3.5 Kaolinite dissolution and precipitation

The concentration of Kaolinite is shown in Figure 32. With the exception of the area of Lavaugrasse is the concentration very low. The point of dissolution is the border between Lavaugrasse and the dike. The chemical formula of kaolinite is $\text{Al}_4[(\text{OH})_8|\text{Si}_4\text{O}_{10}]$.

The base minerals for the formation of kaolinite are feldspar and muscovite. They are easily weathered to kaolinite. An example for this hydrolytic splitting with K-feldspar: First the K^+ is replaced at the mineral surface by H^+ and the K^+ dissolves. Agglomeration of protons results in breaking up of feldspar. As products amorph silica and Kaolinite precipitate.



The alkali and earth-alkali elements are more mobile as aluminum and silica.

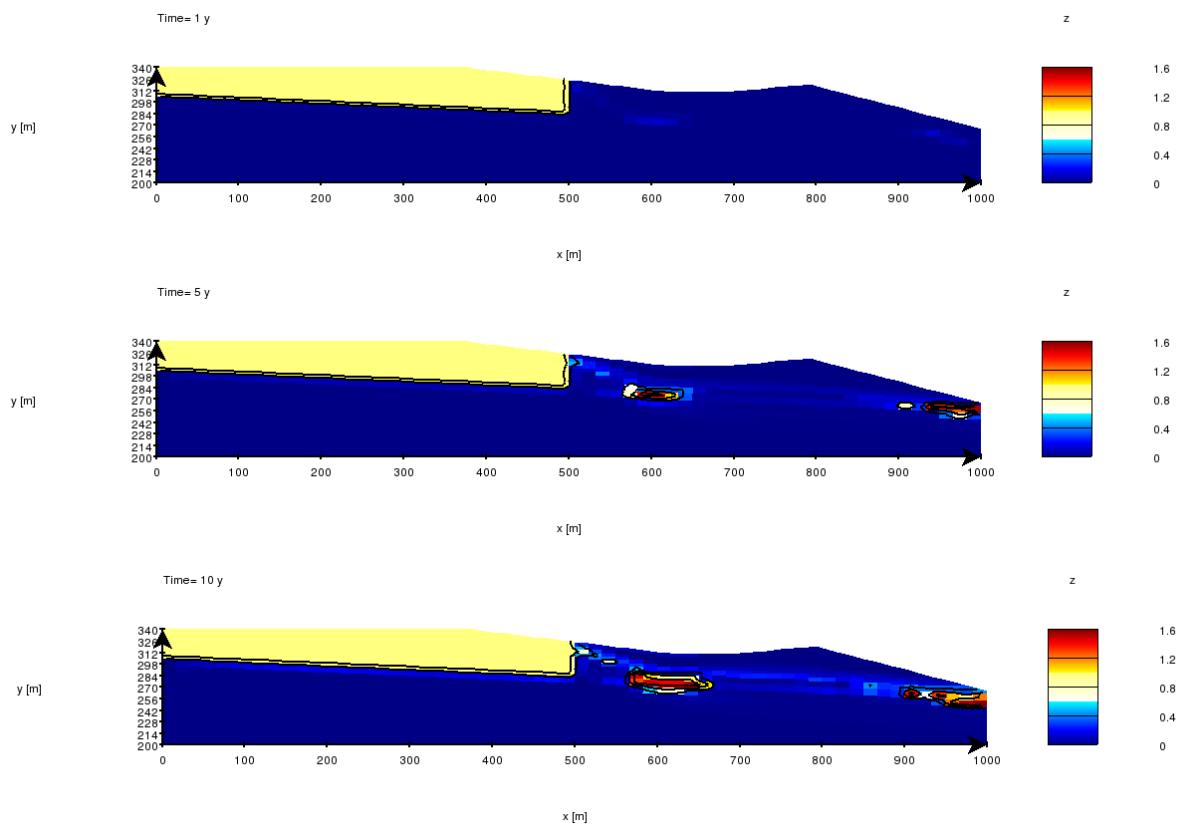


Figure 32: Concentration of the Mineral Kaolinite (mol/l)

4.3.6 Uranium Dioxide (Uranium (IV) Oxide)

The concentration of uranium dioxide as shown in Figure 33 is all over very low and doesn't correlate with the results of the analyses. The concentrations at Figure 33 are for quantitative analysis too low. The dissolution can only be seen in difficulty.

Under reducing conditions dominates UO_2 certainly it is not important for long-distance transportation in groundwater because it precipitates and will be adsorbed at the rocks. In oxidative groundwater uranium dioxide U(IV)O_2 is available as uranyl ion U(VI)_2^{2+} . The hexavalent U^{6+} occurs in nature only in form of $[\text{UO}_2]^{2+}$. This form is easily soluble and binds to complexes with phosphate; sulfate, carbonate and hydroxide in neutral and alkaline conditions. The hydrolyzed uranyl forms are predominant species between pH 4 and pH 7.5. At higher pH complexes with carbonate and hydroxide obtain. The binding behavior depends on pH value, redox potential, availability and temperature. [33] [29]



Dissolved oxygen allows oxidation of uraninite close to the surface and because of the further reducing conditions uraninite reprecipitate. The concentration is very low. The Eh-pH diagram in Figure 26 confirms this circumstance. [26]

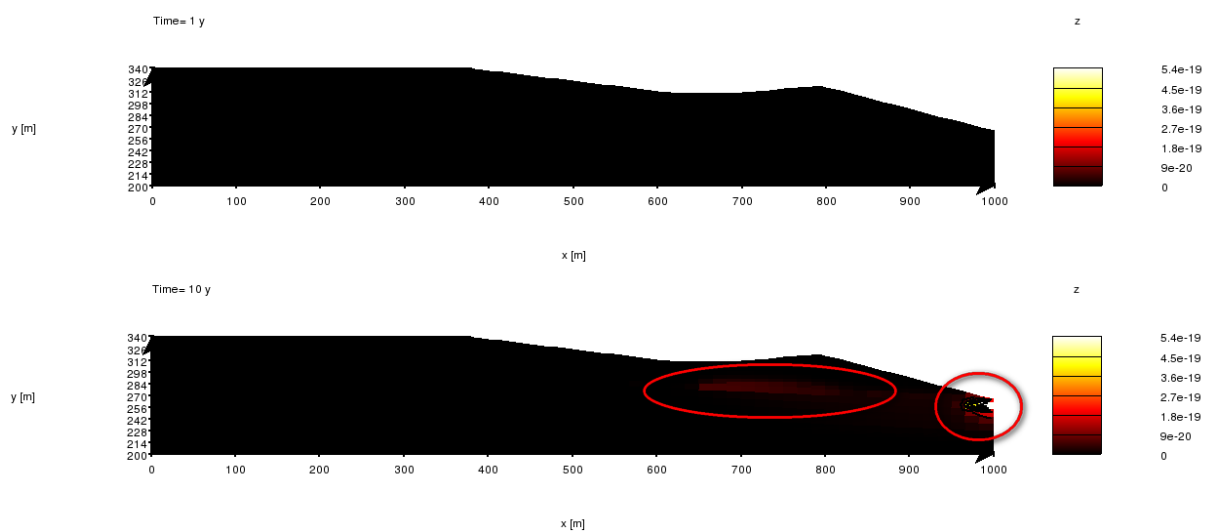


Figure 33: Concentration of Uranium Dioxide (mol/l)

4.3.7 Detailed Examination of a Specific Point

The observed so called “time set point” which is a self-selected observation point in the module which is shown in Figure 34. It is the border of the weathered granite zone to the basin of the river Gartempe.

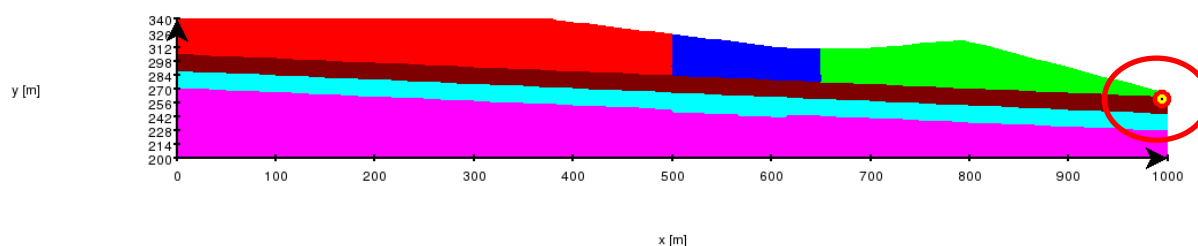


Figure 34: Time Set Point

In Figure 35 the different evolutions of some parameters are shown. The first illustration shows the evolution of (aq) Ca^{2+} ; (aq) Mg^{2+} and (aq) SO_4^{2-} . It can be seen very well that the (aq) Mg^{2+} and (aq) SO_4^{2-} increase very gradually over the ten years. Instead of (aq) Ca^{2+} which makes a sharp turn up between the 4th and 5th year.

The second illustration shows the evolution of (aq) HCO_3^- , (aq) Na^+ and (aq) Al^{3+} . The concentration of (aq) HCO_3^- decreases very gradually a bit and then it remains uniformly. Instead of (aq) Na^+ , its concentration increases slowly and approaches to the (aq) HCO_3^- concentration. The concentration of (aq) Al^{3+} rests poor over the time but increases very progressively. A higher mobilization of (aq) Al^{3+} results of the decreasing pH value.

The third illustration shows the behavior of the minerals kaolinite, fluorite, muscovite and Quartz. The content of muscovite falls rapidly between the 4th and 5th of the simulation. Muscovite is a major mineral and its weathering allows mineral reformation as of kaolinite. Kaolinite increases precisely the opposite case of muscovite. The evolution of quartz is not very stable; it rises and falls over the time. In contrast to fluorite which remains stable until the 6th year, there it starts to fall consequently until the end of simulation.

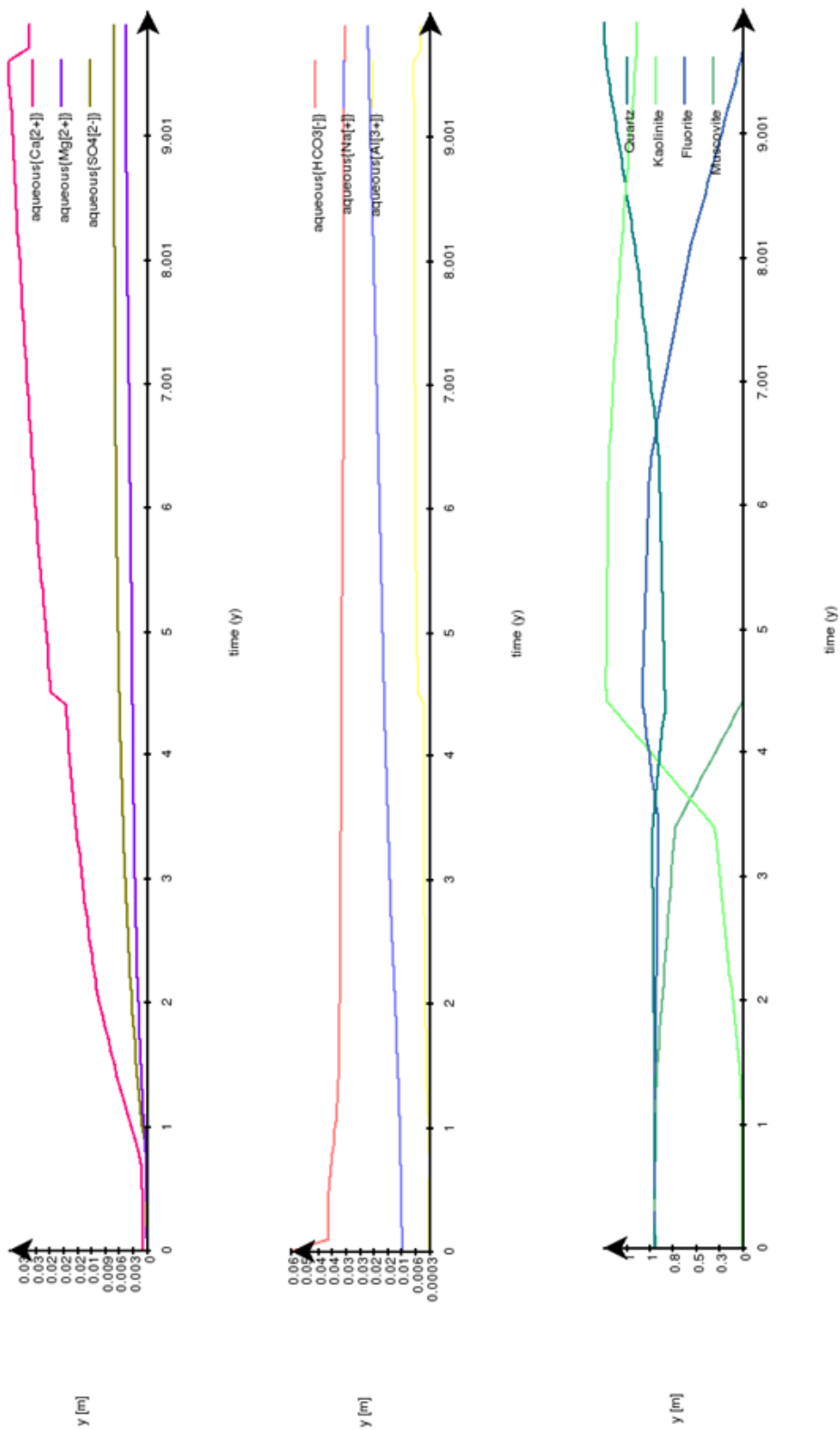


Figure 35: Evolution of Different Parameters at the Time Set Point (concentration in mol/l)

5. Discussion and Conclusion

5.1 Brief Review of the Aim and Structure

The aim of the study was to improve the understanding of the hydrogeochemical behavior of the closed down uranium mining site Bessines-sur-Gartempe next to the village of the same name. The French conglomerate AREVA SA was authorized to do the after care, monitoring and environmental management of this site.

This study was done in three steps, first an on-site sampling to acquire the basic hydrogeological parameters on existing piezometers then chemical analysis of major elements and metals including uranium and radium and as the last step a model with the simulation program HYTEC was created.

5.2 Discussion

This master thesis was focused on heavy metal mobilization but the Acid Mine Drainage serve as a basis for the dissolution of metals. A definition of Acid Mine Drainage is as followed: "Acid Mine Drainage is produced when sulfide-bearing material is exposed to oxygen and water." [34] This takes regularly place in iron sulfide-aggregated rocks as it is given here. This process can happen naturally but mining serves the increasing of the quantity of sulfides exposed. A further definition says that Acid Mine Drainage has "low pH, high specific conductivity, high concentrations of iron, aluminum and manganese, and low concentrations of toxic heavy metals" [34] It can also be noted that the consequences of Acid Mine Drainage are mostly independent of pH and acidity. [34]

The increased input of heavy metals is known caused by anthropogenic activities. Because of the mining activities and the resulting treatment processes increased the possibility of dissolution. At the storages of the study area are waste rocks of static and dynamic leaching treatment deposited. It has to be announced that the decision if a material is waste or an ore depends on several factors particularly the actual metal price and technical availability and complexity of the ore [35]. These materials have higher metal concentrations as the earth crust although they are probably waste. This material contains the primary minerals (weathered sulfides, quartz, feldspar, mica) as well as secondary minerals (gypsum, oxy-hydroxides of iron and clay) and the residues of chemical additives (i.e. sulfuric acid). Precipitation drains into the groundwater body and washes out sulfur and heavy metals. "Waste-rock fast acid solution, whereas tailings may need decades before producing Acid Mine Drainage" [35]. The point is that in waste-rock oxygen can enter more easily which is a question of permeability for water and air. This fast entering of oxygen occurs a fast sulfur oxidation. [35] The weathered parent material granite can contain uranium minerals in particular uranyl-carbonate produced by alteration of uraninite together with iron and clay minerals [36]. This is a possibility which is not characterized for this location.

The concentrations of heavy metals in the samples were as follows $Fe > Mn > U > Zn > Ni$ and the concentrations of the other metals $Ca > Na > Mg > K > Ra$. There is no correlation

between acidic pH and high heavy metal concentrations. The most acidic water samples (pH 3.8) are at SIBGAL with moderate values of Na, K, Mg, Ca, Mn and low levels in Fe, Zn and Ni. SIBGAL has the highest concentrations of Al (14.44 mg/l), U_{sol} (1.07 mg/l) and Ra_{sol} (2.29 Bq/l). In contrast to the highest pH value of PZ98 (pH 6.3), its water samples have the highest concentrations of Fe (300.25 mg/l), Mn (23.94 mg/l), Ca (588.67 mg/l), Mg (163.13 mg/l) and K (28.24 mg/l). This sample contains also the highest concentrations of SO_4^{2-} (2029.61 mg/l), NH_4^+ (8.33 mg/l) and HCO_3^- (456.28 mg/l). The high concentrations of PZ98 can result of the geological composition. Figure 17 shows very well the different composition of this drill hole. Lavaugrasse contains sandy static and dynamic treatment materials with a moderate permeability.

It is very difficult to compare one uranium mining site with another. As mentioned in chapter 1.2 the IAEA distinguishes 12 different types of uranium deposits. The basic conditions are given but every site has its own geological characteristics and a certain interaction with its environment. The basic geochemical conditions are the same but that would be too easy for a comparison. The different values (pH, eh, EC) and concentrations (SO_4^{2-} , HCO_3^- , heavy metals) have a broad variation as well as their interaction.

The results of the simulation show the evolution of different parameters. There the meshing between of geological composition and leaching of ions can be seen. By means of weathering pyrite decreases of the pH and metals dissolve which results in reformation of minerals.

A water treatment is in any case essential because the heavy metal concentrations are part time very high as well as the Ra and U concentrations are over the limit for a direct discharge. The further monitoring and hydro-chemical investigations will still be necessary because the simulation shows that the system is very dynamic and it is difficult to forecast the end of the dissolution of heavy and other metals.

6. Catalogs

6.1 List of References

- [1] *Uranium: the essentials*. Available: <http://www.webelements.com/uranium/> (2013, Sep. 18).
- [2] *Uran – Ressource mit Zukunft*. Available: <http://www.kernenergie.ch/de/uran-ressource.html>.
- [3] *Uraninite Mineral Data*. Available: <http://www.webmineral.com/data/Uraninite.shtml#Ujmrkj9gl4o> (2013, Sep. 18).
- [4] Forschungszentrum Karlsruhe GmbH, *Radioaktivität und Kernenergie*, 2000.
- [5] *Radium: the essentials*. Available: www.webelements.com/radium/ (2013, Oct. 10).
- [6] J.R. Blaise, S. Boitsov, P. Bruneton, M. Ceyhan, F. Dahlkamp, R. Mathie, A. McKay, J. McMurray, J. Slezak, J. Subhash, *World Distribution of Uranium deposits (UDEPO) with Uranium deposit Classification*. Vienna, 2009.
- [7] World Nuclear Association, *World Uranium Mining Production*. Updated July 2013. Available: www.world-nuclear.com/info/Nuclear-Fuel-Cycle/Mining-of-Uranium-Mining-Production/#.UhcV-tJ1ueY (2013, Aug. 23).
- [8] C. Cazala, L. Dewiere, MO. Gallerand, J. Herbelet, AC. Servant-Perrier, "Expertise globale du bilan décennal environnemental d'AREVA NC: 2ème partie: impact environnemental à l'échelle des bassins versants et évaluation de la surveillance," DEI/SARG/2007-042, IRSN - Institut de radioprotection et de sûreté nucléaire, Nanterre, 2007, 2008.
- [9] Ch. Didier, Ed, *The french experience of post mining management*, 2008.
- [10] Ch. Andres, "Les mines d'Uranium en France," Oct. 2009.
- [11] *Wertvolle Erde: Deutsche Bergbaugeschichte*. Available: <http://www.wertvolle-erde.de/suchen-finden-foerdern-und-aufbereiten-von-rohstoffen/deutsche-bergbaugeschichte> (2013, Sep. 18).
- [12] A. Hiller, W. Schuppan, *Geologie und Uranbergbau im Revier Schlema-Alberode*, 500th ed. Dresden: Sächsisches Landesamt für Umwelt und Geologie, 2007.
- [13] V. Devallois, P. Bachaud, "Zone minière de la Crouzille: Etudes hydrogéochimiques de trois sites: Brugeaud - Lavaugrasse - Montmassacrot," Bugeaup Nudex, AREVA NC, Armines, 2010, 2011.
- [14] Th. Doursout, "An overview of uranium mining in France with focus on the Limousin region," Vienna, 2006.
- [15] Ch. Andres, "L'après mine, la R&D en support," Oct. 2008.
- [16] D. Vanden Berghe, P. Bachaud, "Modélisations hydrogéologiques 3D du sites de Bessines-sur-Gartempe et Montmassacrot," Jan. 2012.
- [17] Grundfos, *MP1 stainless steel submersible pumps for environmental purge and sampling applications: Installation and operating instructions*, 2002,2011.
- [18] N. Martineau, "étalons de l'analyse", e-mail, Sep. 2013.
- [19] unknown, *Méthode IC*.
- [20] A. Berland, "L'analyse du radium et uranium", e-mail, Oct. 2013.

- [21] *Natural uranium and the environment: Radionuclid sheet*. Available: <http://www.irsn.fr/EN/Research/publications-documentation/radionuclides-sheets/environment/Pages/Natural-uranium-environment.aspx> (2013, Oct. 13).
- [22] J. van der Lee, L. De Windt, V. Lagneau, P. Goblet, "Module-oriented modeling of reactive transport with HYTEC," in *Computer & Geosciences*, pp. 265–275.
- [23] UIS Commission on Karst Hydrogeology and Speleogenesis, IAH Commission on Karst Hydrogeology, *Glossary of Karst and Cave Terms: hydrodynamic dispersion*. Available: <http://www.speleogenesis.info/directory/glossary/?term=hydrodynamic%20dispersion> (2013, Oct. 02).
- [24] E. Ledoux, J.M. Schmitt, "Etude du fonctionnement hydrogéochimique de l'ancien site minier de Bellezane: (Limousin, France)," No R100119EL, BGM/DGS RT 10/004, Ecole des mines de Paris, Fontainebleau (Centre de Géosciences), France, 2004.
- [25] L. De Windt, "Modélisation géochimique appliqué aux problèmes d'environnement," Master 2, Hydrogéologie/Hydrochimie, Janvier 2012. Centre de Géoscience, Mines ParisTech, Fontainebleau, France, 2012.
- [26] V. Lagneau, "Concentration très bas de l'uranium", e-mail, Oct. 2013.
- [27] Ch. Vornehm, *Hydro-geochemische Untersuchungen zum System Niederschlag-Boden-Grundwasser im Grundgebirge des Bayerischen Waldes*. Dissertation an der Fakultät für Geowissenschaften der Ludwig-Maximilians-Universität München, 2004.
- [28] Laboratorium zur Bestimmung von Isotopen in Umwelt und Hydrogeologie, *Uran und Radium im Grund- und Mineralwasser*. Available: www.hydroisotop.de (2013, Nov. 06).
- [29] M. Gavrilesco, L. Pavel, I. Cretescu, "Characterization and remediation of soils contaminated with uranium," in *Journal of Hazardous Materials*, pp. 475–510.
- [30] A.M. Giblin, B.D. Batts, D.J. Swaine, "Laboratory simulation studies of uranium mobility in natural waters," in *Geochemica et Cosmochimica*, pp. 699–709.
- [31] N. Rapantova, M. Licbinska, O. Babka, A. Grmela, P. Pospisil, "Impact of uranium mines closure and abandonment on groundwater quality," in *Environmental Science Pollution Research*, pp. 7590–7602.
- [32] H.W. Kirby, M.L. Salutsky, *The Radiochemistry of Radium: Nuclear Science Series*. National Academy of Sciences, 1964.
- [33] R. Goulet, C. Fortin, D. Spry, *Uranium*, 2012.
- [34] A. Akcil, S. Koldas, "Acid Mine Drainage (AMD): causes, treatment and case studies," in *Journal of Cleaner Production*, pp. 1139–1145.
- [35] B. Dold, "Sustainability in metal mining: from exploration, over processing to mine waste management," in *Reviews in Environmental Science and Biotechnology*, pp. 275–285.
- [36] S. Singh, M. Hendry, "Solid-Phase Distribution and Leaching Behaviour of Nickel and Uranium in a Uranium Waste-Rock-Piles," in *Water Air Soil Pollution*

6.2 List of Abbreviations

AAS	Atom Absorption Spectroscopy
AD	Anno Domini
AMD	Acid Mine Drainage
BC	Before Christ
D711	Route Départementale (Country Road)
DGEC	Direction Générale de l'Energie et Climat
DGPR	Direction Générale de la Prévention des Risques
DPPR	Direction de la Prévention des Pollutions et des Risques
IAEA	International Atomic Energy Agency
IC	Ion Chromatography
ICP-AES	Inductively Coupled Plasma – Atomic Emission Spectroscopy
ICP-MS	Inductively Coupled Plasma – Mass Spectroscopy
ICRP	International Commission on Radiological Protection
ISL/ISR	In Situ Leach
NGF	Nivellement Général de la France
RGIE	Règlement Général des Industries Extractives
TAETA	Taux Annuel d'Exposition Totale Ajoutée
TDS	Total Dissolved Solids
VAC	Voltage in Alternating Current

6.3 List of Tables

Table 1: Maximum permissible values of Ra-226 and U-238 for drinking water [8].....	7
Table 2: Ra-226 and U-238 limits of the circular letter of the 9 th march 1990 [8].....	8
Table 3: Permeability of the different types of granit [13]	14
Table 4: Results of the analysis of the solid residues of the dynamic treatment [13].....	16
Table 5: Ranges of permeability of the backfilling material [13]	16
Table 6: Average temperature (°C) in Bessines-sur-Gartempe [8].....	18
Table 7: storage and stock pile data [13].....	24
Table 8: Data of the pumping	37
Table 9: Monoelement Standard [18].....	38
Table 10: Measurement conditions liquid ion chromatography [19].....	41
Table 11: Different standards for the IC [18].....	41
Table 12: Basic geological parameters for the simulation [16]	45
Table 13: Minerals in equilibrium	46
Table 14: Composition of the rain at the Massif Central [25].....	46
Table 15: Results of the on-site analysis in Bessines (T... Temperature, EC... Electrical Conductivity, DO ... Dissolved Oxygen, Eh...Redox Potential).....	47
Table 16: Results of the analysis of the laboratory of the Centre de Géoscience in Fontainebleau	49
Table 17: Comparison of samples	50
Table 18: Results of the analysis of the laboratory of AREVA next to the closed mining site in Bessines-sur-Gartempe.....	52

6.4 List of Figures

Figure 1: Uranium-Radium Radioactive Series [4]	4
Figure 2: World uranium production and demand [7]	6
Figure 3: Uranium exploitation in France [10]	9
Figure 4: Localization of the sites inside the Crouzille Division [14]	12
Figure 5: Average rainfall Bessines-sur-Gartempe 1996-2011 [8]	17
Figure 6: Annual rainfall Bessines-sur-Gartempe 1996-2011 [8].....	18
Figure 7: Open pit mining site of Brugeaud in 1955 [10]	20
Figure 8: Area of the Industrial Site of Bessines	22
Figure 9: Ancient hydrographic network [13].....	26
Figure 10: symbol icon of Lavaugrasse [10]	28
Figure 11: shows the hedging of the storage of residues. The different layers provide as mechanical and radiological protection. Figure 11 Reinforcement of dikes, hedging (First layer... Residues with a welded wire mesh, second layer ... protection structure against radioactive transports, third layer ... barren rock) [10]	28
Figure 12: Mining Site Bessines-sur-Gartempe in 1978 (TMS... underground mining; MCO... open pit mining) [10].....	29
Figure 13: Mining Site Bessines-sur-Gartempe after reclamation in 2001 [10].....	29
Figure 14: Location and numeration of measurement and sampling sites.....	31
Figure 15: Look at the basin Vieux Moulin [16]	31
Figure 16: the equipment for the pump MP1 and the pump MP1 [17]	32
Figure 17: Depth profile in the drill hole PZ98 [16]	33
Figure 18: Depth profile in the drill hole PZ95 [16]	34
Figure 19: Depth profile in the drill hole PZ96/PZ96B [16]	35
Figure 20: Depth profile in the drill hole PZ94 [16]	36
Figure 21: AAnalyst 300 Perkin Elmer	39
Figure 22: LC DIONEX DX 500 with the gradient pump GP40 and the electrochemical detector ED40	40
Figure 23: Global structure of HYTEC and related simulation tools based on CHESS [22] ...	43
Figure 24: Simulation profile	44
Figure 25: Details of the model section. (red: Lavaugrasse, residues; blue: Dike, residues; green: Vieux Moulin, waste piles; brown: weathered granite; light blue: fractured granite; pink: unaltered granite).....	45

Figure 26: Eh-pH-diagram of uranium and its species $U^{4+} = 0.01$ mg/l, $T = 12^{\circ}C$, $P = 1.013$ bars, $a[\text{main}] = 10^{-1.88}$, $a[\text{H}_2\text{O}] = 1$, $a[\text{SO}_4] = 10^{1.89}$, $a[\text{HCO}_3] = 10^{2.26}$ [31]	51
Figure 27: Piper-diagram of the water samples	53
Figure 28: Flow Rate (m/s)	54
Figure 29: Evolution of the pH value	55
Figure 30: Evolution of the Sulfate Ion (mol/l)	56
Figure 31: Concentration of Muscovite (mol/l)	57
Figure 32: Concentration of the Mineral Kaolinite (mol/l)	58
Figure 33: Concentration of Uranium Dioxide (mol/l)	59
Figure 34: Time Set Point	60
Figure 35: Evolution of Different Parameters at the Time Set Point (concentration in mol/l) ..	61